Designing Synthetic Biomolecular Condensates in Bacteria

by

Sara Elizabeth Whitlock

B.S., John Brown University, 2016

Submitted to the Graduate Faculty of the

Dietrich School of Arts and Sciences in partial fulfillment

of the requirements for the degree of

Master of Science

University of Pittsburgh

2020

UNIVERSITY OF PITTSBURGH

DIETRICH SCHOOL OF ARTS AND SCIENCES

This thesis was presented

by

Sara Elizabeth Whitlock

It was defended on

November 25, 2020

and approved by

Jeffrey L. Brodsky, Professor, Department of Biological Sciences

Arohan Subramanya, Associate Professor, Department of Medicine

Kabirul Islam, Assistant Professor, Department of Chemistry

Thesis Advisor: W. Seth Childers, Assistant Professor, Department of Chemistry

Designing Synthetic Biomolecular Condensates in Bacteria

Sara Elizabeth Whitlock, M.S.

University of Pittsburgh, 2020

Despite lacking many of the organelles possessed by eukaryotes, bacteria are able to localize important enzymes and signaling proteins to specific subcellular locations. One way that bacteria accomplish this localization is through the formation of phase separated membraneless organelles called biomolecular condensates. These structures are composed of proteins and RNA and they self-assemble into multimeric networks, bind client proteins, and recruit them to particular locations within the cell. This thesis describes the history of biomolecular condensates and the design of synthetic mimics of bacterial biomolecular condensates.

Chapter one details the proposed connection between biomolecular condensates and the earliest forms of life on earth. I trace the history of biomolecular condensates starting with the 1924 proposal that complex coacervates—similar to modern biomolecular condensates—were the first forms of life. I then follow the modernization of this idea after decades of ridicule, describing the first discovery, in *C. elegans*, of a coacervate-like structure operating within the cells of a modern organism. This discovery led to the characterization of biomolecular condensate structures throughout the eukaryotic cell and, in 2018, to the discovery of a biomolecular condensate in bacteria.

With several bacterial condensates now described, I propose in chapter two a strategy for designing synthetic biomolecular condensates in bacteria. These designs are inspired by the pole organizing protein Z (PopZ) of *Caulobacter crescentus*, which forms a unipolar biomolecular condensate when expressed in *Escherichia coli*, and by a series of peptide hydrogels designed for

cell encapsulation and drug delivery. I use these synthetic constructs to define the minimal domains necessary to form a pole-localized scaffold and demonstrate the impact that varying charge, amount of disorder, and degree of multivalency has on synthetic condensate formation. I recruit and exclude client proteins from synthetic condensates, and I propose ways to use these designs to set up asymmetric division of biomolecular condensates in *E. coli*.

Overall, this thesis contributes to the understanding of how bacterial biomolecular condensates localize to the pole and develops strategies to mimic this behavior with synthetic condensates.

Table of Contents

List of Tables

List of Figures

Preface

My heartfelt thanks go to all those without whom this thesis wouldn't exist.

To my mentor Seth Childers. I think of the words of Adrienne Rich, that "one can teach others to think only in the sense of appealing to and fostering powers already active in them." Thank you for seeing what I was capable of, for fostering my scientific mind, and for giving me so much support as I found my path, even if that path wasn't exactly what we expected when we set out on this journey together.

To my parents, who love learning, who sacrificed to provide me with every opportunity, and who listened sympathetically to every high and low along the way.

To my close friends, whose intellect and desire for truth inspire me, and who provided so much perspective and camaraderie.

1.0 Biomolecular Condensates: From Origins of Life to Synthetic Biology

This chapter was inspired by an article previously published in Scientific American: In Search of Life's Beginnings, by Sara Whitlock

1.1 Introduction

For millennia, ideas about the origin of human life were purview of the divine. Because such ideas were not were testable, natural scientists did not investigate these questions. Then, Aleksandr Oparin quietly published a pamphlet describing a theory for the chemical origin of life that contained sufficient detail for experimental study.[1] Relatively soon after the book's English translation, it was clear that two components of Oparin's theories were prescient—that the early atmosphere of earth was reducing in nature and that the first organisms were heterotrophs relying on an external soup of nutrients for metabolism.[2]

Stanley Miller and Harold Urey tested and confirmed Oparin's primordial soup idea in a classic 1953 experiment. Applying an electric current to water, hydrogen, methane and ammonia in a "primordial earth" atmosphere, they observed the formation of amino acids and complex macromolecules within a week.[3] This demonstrated that under Oparin's proposed early-earth conditions, the spontaneous formation of life-building molecules would have been possible.

Another of Oparin's ideas about the origin of life didn't share early acceptance. He also proposed that the first living systems on earth were complex coacervates—associations of water-soluble, oppositely charged macroions which phase-separate when they

approach neutrality (Figure 1).[1,2,4,5] This idea was widely discussed upon its translation into English in 1938; however, with the discovery of DNA as the genetic material Oparin's ideas were discarded.[6,7] His coacervates were largely proteinaceous, and thus their utility in a nucleotide-based system of genetic information storage was unclear for many years.[2,6]

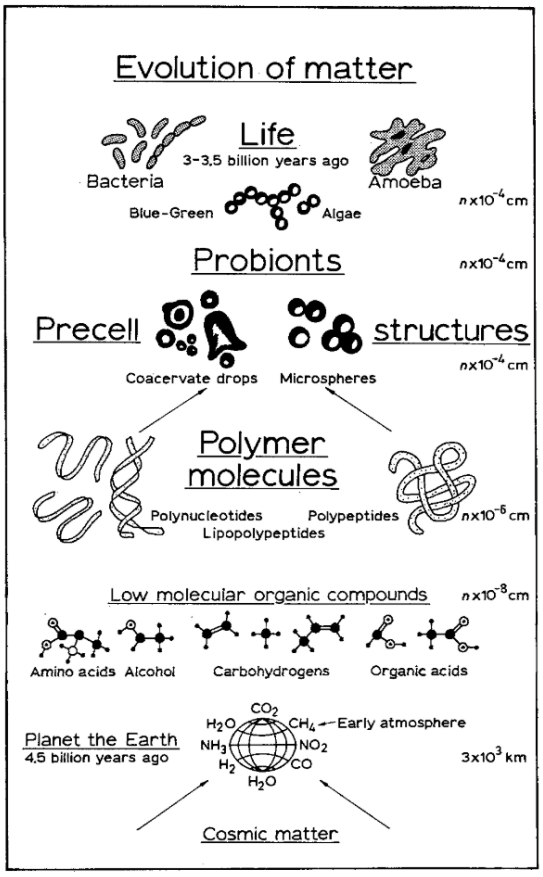

Figure 1: Early scheme for coacervates in the origin of life. A figure showing coacervate pre-cell structures as in intermediate stage in the evolution of life. This predates the modern era, in which biomolecular condensates are once again included in the trajectory of the evolution of life. Reprinted by permission from Springer Nature: Origins of Life 5(1–2),201–205, Coacervate Systems and the Origin of Life, T. Evreinova et al., 1974.

Oparin later contended that the status of DNA as the primary genetic material did not change his idea of coacervates as the first life forms. The repeated, rapid formation and dissolution of these phase separated systems—in solutions containing nucleic and amino acids—allowed for the polymerization of each type of acid. This, he said, allowed for natural selection to shape these

preliminary genes and proteins simultaneously, without any chicken-and-the-egg conundrums concerning the order of appearance of first genetic material or the enzymes catalyzing its replication. [1,8]

The Cold War further dampened enthusiasm for Oparin's ideas. As a scientist steeped in Marxist philosophy, Oparin was disregarded by US scientists at a time when fear of Marxism was powerful[6]. In this atmosphere, even his continued assertions that coacervates were the earliest life forms were ignored by biologists for many years as they turned to DNA—and later lipid-bound vesicles—in their discussion of early life.[6,8]

1.2 Early Expansion of Coacervate Concepts by Fox and Bahadur

At this point, chemists took up the idea of complex coacervates as the earliest life forms. Sydney Fox, an American biochemist, built upon Oparin's creation of prototype phase-separated early life forms. Where Oparin had built protocells out of modern proteins like gelatin, Fox focused on using abiotic polypeptides with a diverse mix of amino acids of the variety that might have formed as life began—building on the work of Miller and others who showed formation of amino acids in early-earth conditions (Figure 2A,B).[3,9] Using his newly created abiotic polypeptides, Fox demonstrated thermal formation of proteinoid microspheres at plausible early-earth temperatures.[9] After a heating and cooling cycle, Fox's abiotic polypeptides assembled into spherical structures approximately the size of coccoid bacteria, and they demonstrated characteristic phase-separation behaviors such as changing their size in response to varying ionic strength[9].

Across the world from Fox, a chemist in India at the University of Allahabad was performing similar experiments. Krishna Bahadur published about small particles he called

'Jeewanu' throughout the 1960s. This name comes from Sanskrit words meaning 'the particle of life,' and Bahadur prepared them by combining a carbon source, like citric acid, inorganic catalysts such as colloidal molybdenum or iron oxides, and minerals, then shaking the solution under sunlight—a contrast to Fox's thermally prepared proteinaceous spheres (Figure 2C).[10,11] Bahadur's solution—left to its own devices for several days in the sun—formed first amino acids, then peptides, and finally proteinaceous globules of 'jeewanu,' and he reported seeing these particles exhibit phase behaviors including expanding in size and splitting in two.[10]

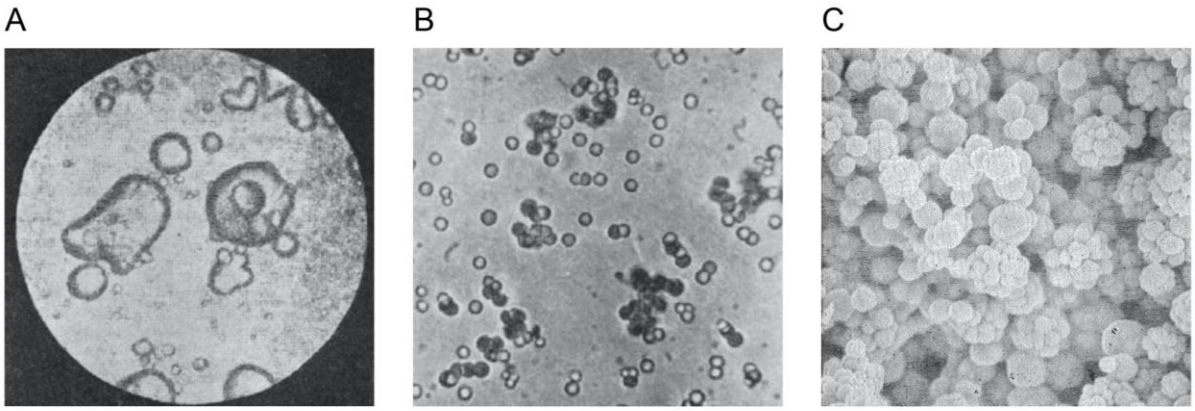

Figure 2: Early studies of coacervates *in vitro* (A) Oparin's coacervate droplets composed of gelatin, gum arabic, and ribonucleic acid. At x240 magnification. (B) Fox's protenoid microspheres, formed by allowing a hot solution of polyamino acid protenoid to cool. Microspheres are ~2 μm in diameter. (C) Bahadur's Jeewanu particles, shown at x2000 magnification. Figure adapted with permission from Springer Nature: Nature 205(4969), 328–340, S. Fox, A Theory of Macromolecular and Cellular Origins, 1965 and Springer Nature: Journal of Biosciences, Vol. 36, Issue 4, pp. 563–570, Mathias Grote, Jeewanu, or the 'particles of life:' the approach of Krishna Bahadur in 20th century origin of life research, 2011.

Though his experiments did bear similarity to Fox's, philosophical and cultural differences kept Bahadur from gaining acceptance with his research contemporaries. He believed his particles were fully alive, working under a different definition of life than Western scientists, and didn't thoroughly record details of the composition of jeewanu.[10] For these—partially valid—reasons,

Bahadur's work was criticized, dismissed from the cannon of work on the origins of life, and largely forgotten.[10,12]

Despite both men's work to expand Oparin's ideas of coacervates as the earliest evolutionary stage of life and demonstrate the geophysical viability of protein-based coacervate formation in early evolution, their link to modern biological systems remained unclear for many years. Examining modern cells and seeing intricate, lipid-bound membranes and meticulously packaged DNA did not indicate to biological researchers that solely proteinaceous systems could have birthed such complexity.[2]

1.3 Modern Era of Biomolecular Condensates

Oparin's coacervate hypotheses continued to be ignored until 2009, when Clifford Brangwynne made a surprising discovery while studying the common laboratory model organism *C. elegans*. He was examining structures called p granules, which are part of the system by which *C. elegans* embryos specify the germ cells that will eventually go on to produce eggs and sperm[13]. At the time, it was unknown how p granules—which contain both RNA and RNA-binding proteins—localize to the posterior half of a single cell embryo before its first division into a somatic cell and a germ cell. This positioning is critical for designating the posterior end as the embryo's first germ cell, and any p granules left at the anterior end of the cell are degraded.[14]

Having seen a cytoplasmic flow moving toward the posterior end of the embryo before division, Brangwynne began his experiments with the hypothesis that p granules are solid nuggets pushed by this flow to the posterior end (Figure 3A).[13,15] Alternatively, he thought, it was possible that p granules were completely degraded at the anterior end of the embryo and reassembled at the

posterior end.[13] If solid p granules were moving via cytoplasmic current towards the anterior end of the cell, Brangwynne and his colleagues reasoned it should be possible to tag key proteins of the p granule with green fluorescent protein (GFP) and watch them move towards the anterior end using three-dimensional particle tracking. They did so with the p granule proteins PGL-1 and GLH-1, and instead found p granules moving towards both the anterior and posterior ends of the embryo (Figure 3B).[13]

To further investigate p granule localization, they inhibited the embryo's ability to break symmetry—keeping it from initiating the asymmetric division into germ cell and somatic cell—using RNA interference of a centrosomal protein called SPD-5. As soon as they relaxed interference and the embryo broke symmetry, p granules seemed to appear out of nowhere—and only at the posterior end (Figure 3C).[13] This observation was crucial because it pointed to a phase transition from a soluble form to a condensed liquid in the formation of p granules—and indicated that area-specific concentration of granule components was responsible for their anterior localization in the embryo. Together with their observation that p granules appeared to occasionally fuse together, Brangwynne and colleagues decided to pursue the idea of liquid, phase-separated p granules.

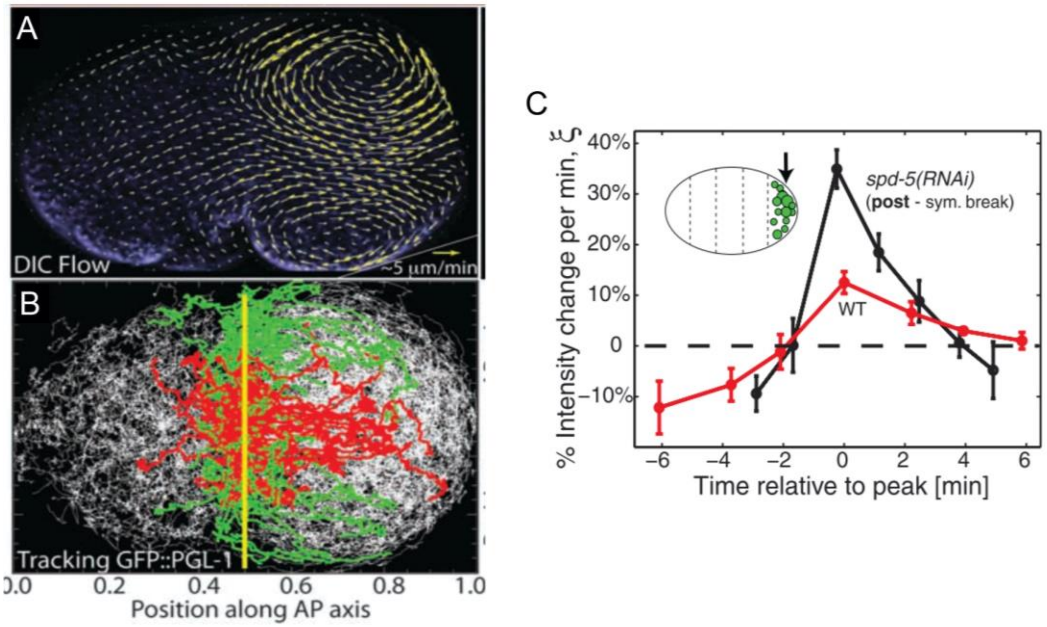

Figure 3: *C. elegans* P granules form independent of cytoplasmic flow (A) Cytoplasmic flow analysis of a single *C. elegans* embryo (blue DIC image) during symmetry breaking. Yellow arrows indicate flow direction and magnitude. (B) Overlay of P granule trajectories (white) from five GFP::PGL-1 embryos. Trajectories crossing into the posterior are shown in red, and those crossing into the anterior are in green. (C) The growth rate of P granules in the embryo posterior (arrow) after complete P granule dissolution in spd-5(RNAi) GFP::PGL-1 embryos. From Brangwynne, C. P et al. (2009). Germline P Granules Are Liquid Droplets That Localize by Controlled Dissolution/Condensation. Science, 324(5935), 1729–1732. Reprinted with permission from AAAS.

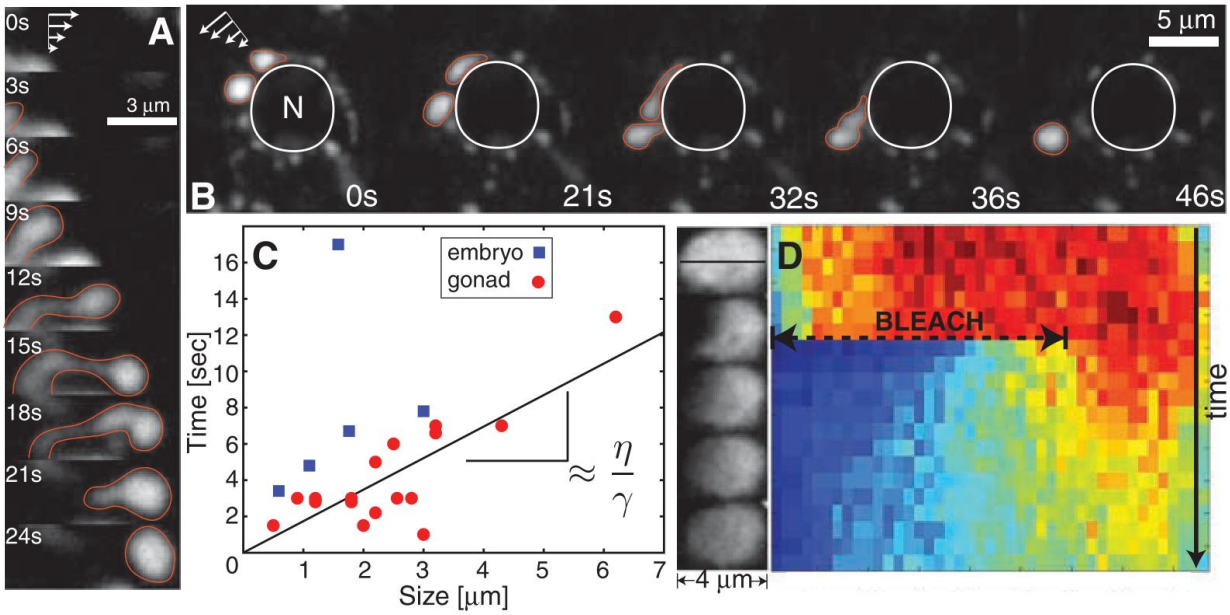

Figure 4: *C. elegans* P granules behave like liquids (A) Jetting P granule (red outline) from a dissected GFP::PGL-1 germ- line nucleus (lower left, not visible). Shear direction, white arrows. (B) Dripping P granules (red outline) from a dissected GFP::PGL-1 germ line. Nucleus (N), white line. (C) Time scale of drop breakup and fusion events in dissected germline and early embryos, as a function of droplet size. The black line is a linear fit, yielding a ratio of viscosity to surface tension (h/g) ≈ 2s/mm. (D) Fluorescence recovery after photobleaching (FRAP) of a large nuclear-associated GFP::PGL-1–labeled P granule from an eight-cell embryo (upper left sequence; top to bottom = 20s). Kymograph is along the black line in left sequence. Red denotes high intensity and blue, background intensity. The intensity decreases in the unbleached region (fluorescence loss in photobleaching, FLIP) as the bleached region recovers. From exponential fits, in the bleached region tFRAP = 4.7 s, and in the unbleached region tFLIP = 5.7s. From Brangwynne, C. P et al. (2009). Germline P Granules Are Liquid Droplets That Localize by Controlled Dissolution/Condensation. Science, 324(5935), 1729–1732. Reprinted with permission from AAAS.

They used two methods to demonstrate the liquid nature of p granules: application of shear stress and fluorescence recovery after photobleaching (FRAP). When a stress was applied to p granules associated with the nucleus of a worm cell, the p granules slid down the side of the nucleus, dripping and fusing together as expected for a liquid (Figure 4 A, B, C).[13] When the group

bleached the center of a p granule containing the same PGL-1-GFP fluorescent fusion protein used in earlier experiments to track the granule through the embryo, they saw quick recovery—in the timescale of seconds—of the fluorescence of the bleached area, consistent with previous measurements of the fluorescence recovery of viscous liquids like glycerol (Figure 4D).[13] Both results further demonstrated that p granules behave as phase-separated liquids in the *C. elegans* embryo.

With this set of experiments, Oparin's coacervates entered the 21st century cell. Here, a structure much like the one Oparin predicted, with soluble, charged molecules that phase separates from its surroundings, was operating in a modern cell. Immediately, Brangwynne connected the discovery of this new type of cytoplasmic structure both as a possible organizing mechanism for similar cellular bodies containing RNA and proteins—like P bodies, Cajal bodies, and stress granules—and as a mechanism of self-assembly for early life forms.[13]

1.4 Correlation of Low Complexity Sequences and Multivalency with Phase Separation

Further investigations into RNA granules—the name for the family of RNA/Protein structures to which p granules belong—revealed that Brangwynne was right about the abundance of phase-separated structures in the cytoplasm. In 2012, Kato et al. were studying compounds predicted to induce mouse stem cell differentiation into cardiomyocytes when they realized that a compound called b-isox (formally 5-aryl-isoxazole-3-carboxyamide) selectively precipitated a group of proteins implicated in neurodegenerative diseases—many of which were members of neuronal RNA granules.[16]

To determine which features of these proteins allowed them to precipitate with the b-isox compound, the group created a series of fusion proteins from seven members of the precipitate. They found that the sections of these proteins causing them to precipitate with the b-isox compound were low complexity (LC) sequences.[16] These are sections of protein containing repeats of single amino acids or short amino acid motifs. Furthermore, the group observed that the LC sequence sections of the precipitated proteins were able to phase separate, both when isolated and in association with previously formed hydrogels. This phase-separation ability was only reduced when the numbers of tyrosine residues—which featured prominently in a low-complexity motif shared among the RNA granule proteins—were decreased by mutation to serine.[16]

This work greatly expanded the pool of known, modern cellular structures that behave as Oparin predicted. The phase-separated p granules Brangwynne studied in worms have relatives in mouse stem cells—and with Kato et al.'s insight into mechanistic details of phase-separation, the field was open for discovery of similar phase-separated structures.

At the same time, Michael Rosen's group explored another facet of the mechanisms of phase transition. Drawing from polymer chemistry, the group knew that both the number of interactions—called the valency—between molecules capable of forming a gel as well as the strength of those interactions determines the transition point between soluble and gel states. Seeking to understand if these rules also guide phase transitions inside eukaryotic cells, they constructed a set of synthetic molecules: one featuring variable numbers of repeats of the SH3 signaling domain and the other with varying numbers of an SH3 binding partner, PRM (Figure 5A).[17] Both proteins had repeats of their respective domains separated by flexible linkers. Combining these proteins *in vitro*, they found a phase transition to a gel-like state occurred for molecules with repeats of four binding units or more, with a greater concentration of molecules

moving into the phase-separated assembly as the number of binding units increased (Figure 5 B, C).[17]

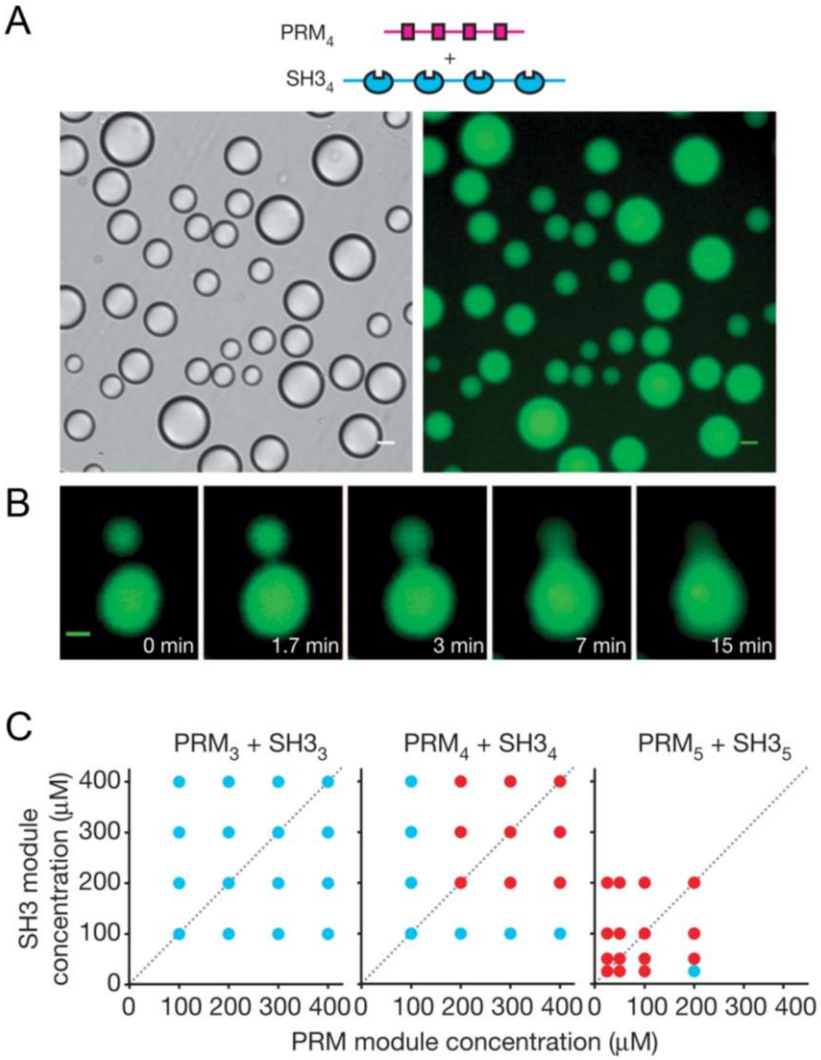

Figure 5: Multivalency impacts phase behavior of condensates (A) Domain architecture of the PRM_4 and $SH3_4$ constructs, with folded domains separated by flexible linkers. Bellow, liquid droplets observed by differential interference contrast microscopy (left) and wide-field fluorescence microscopy (right) when 300 μM $SH3_4$, 300 μM PRM_4 (both of which are module concentrations; molecule concentrations are 75 μM) and 0.5 μM OG–$SH3_4$ were mixed. Scale bars, 20 μm. (B) Time-lapse imaging of merging droplets that were formed as in (A). Scale bar, 10 μm. (C) Phase diagrams of multivalent SH3 and PRM proteins. The concentrations are in terms of the modules. The red circles indicate phase separation, and the blue circles indicate no phase separation. Reprinted by permission from

They also observed valency-dependent phase separation behavior *in vivo*. The SH3/PRM synthetic partner set formed phase separated droplets in HeLa cells when the $SH3_5$/PRM_5 constructs containing five binding units were expressed, but did not when $SH3_5$ was instead expressed with the shorter PRM_3 construct.[17] Furthermore, the group demonstrated dependency of a native three-component signaling system composed of the proteins nephrin, NCK, and N-Wasp on both presence of all components of the system and on phosphorylation of the nephrin protein. Phosphorylation of the protein changes the effective valency of nephrin, thereby demonstrating a mechanism by which such systems might be regulated *in vivo*.[17]

1.5 The Emergence of Biomolecular Condensates as a Fundamental Compartmentalization Strategy

With the importance of these mechanistic details of *in vivo* coacervates established—that proteins contain low complexity sequences of amino acids and have multivalent interactions—the field exploded. Today, phase-separating structures have been found throughout the eukaryotic cell—from the nucleolus and Cajal bodies in the nucleus to p bodies, stress granules, and germ granules in the cytoplasm—and the group of these structures is collectively referred to as biomolecular condensates (Table 1). They are defined as micron-scale compartments in eukaryotic cells that lack surrounding membranes but function to concentrate proteins and nucleic acids.[18]

Table 1: Eukaryotic biomolecular condensates and their function. Adapted with permission from Springer Nature, Banani, S. F. et al. (2017). Biomolecular condensates: Organizers of cellular biochemistry. Nature Reviews Molecular Cell Biology, 18(5), 285–298**.**

Body	Alternative names/examples	Localization	Function
P-body	Processing body, GW body, decapping bodies	Cytoplasm	mRNA decay, mRNA silencing
U-body	Uridine-rich snRNP body	Cytoplasm	Storage/assembly of snRNPs
Balbiani body		Cytoplasm, germ cells	Storage
Germ granules	P-granule, nuage, chromatoid bodies, Balbiani body	Cytoplasm, germ cells	Storage?
RNA transport granules	neuronal RNA granule	Cytoplasm, neurons	mRNA storage/transport
Synaptic densities	Postsynaptic densities	Cytoplasm, neurons	Neurotransmission
Stress granule	NA	Cytoplasm, upon stress	Translational regulation/mRNA storage
Nuclear pore complex	NA	Nuclear membrane	Nuclear import/export
Cajal body	NA	Nucleus	Assembly and/or modification of splicing machinery
Cleavage body	NA	Nucleus	mRNA processing
Gem	Gemini of Cajal bodies	Nucleus	Storage?; aid histone mRNA processing
Nuclear speckles	splicing factor compartments (SF compartments), interchromatin granule clusters (IGCs), B snurposomes	Nucleus	mRNA splicing
Nucleolus	NA	Nucleus	Ribosome biogenesis
OPT domain	NA	Nucleus	Transcriptional regulation
PcG body	Polycomb group bodies	Nucleus	Transcriptional repression
Perinucleolar compartment	NA	Nucleus	Associated with malignancy
PML bodies	nuclear domain 10 (ND10), Kremer bodies, PML oncogenic domains	Nucleus	Transcriptional regulation; apoptosis signaling; antiviral defense
Histone locus body (HLB)	NA	Nucleus	Histone mRNA biogenesis
Paraspeckles	NA	Nucleus	RNA processing?
Focal adhesions	NA	Plasma membrane	Cell adhesion/migration
Nephrin clusters	NA	Plasma membrane	Glomerular filtration barrier
TCR clusters	NA	Plasma membrane	Immune synapse
Podosomes	NA	Plasma membrane	Cell adhesion/migration
Actin patches	NA	Plasma membrane	Endocytosis

Studying the many eukaryotic biomolecular condensates reinforces initial observations of the importance of multivalent interactions and low complexity sequences in phase-separating systems, as well as providing additional mechanistic details. For the condensates observed to phase separate via multivalent interactions, having a higher number of interactions and a greater binding affinity between interactions enables larger structures to form at lower concentrations.[18] Building off this observation, for those condensates that phase separate via their intrinsically disordered regions, researchers observe that the sequences of those disordered regions often feature positively and negatively charged amino acid blocks that facilitate phase separation behavior, creating many small points of interaction that mimic the multivalent interacting motifs of the previous category.

One example of this type of charge block-driven phase separation is the protein responsible for formation of the nuage/chromatid body family of biomolecular condensates. This type of condensate forms in developing sperm cells and contains proteins that are responsible for preventing damage to spermatocytes or spermatids by transposable genetic elements.[19] The protein responsible for nuage condensate formation, Ddx4, contains alternating blocks of positively and negatively charged amino acids in its N-terminal disordered region, and scrambling the sequence of these amino acids prevents formation of nuage condensates (Figure 6).[19]

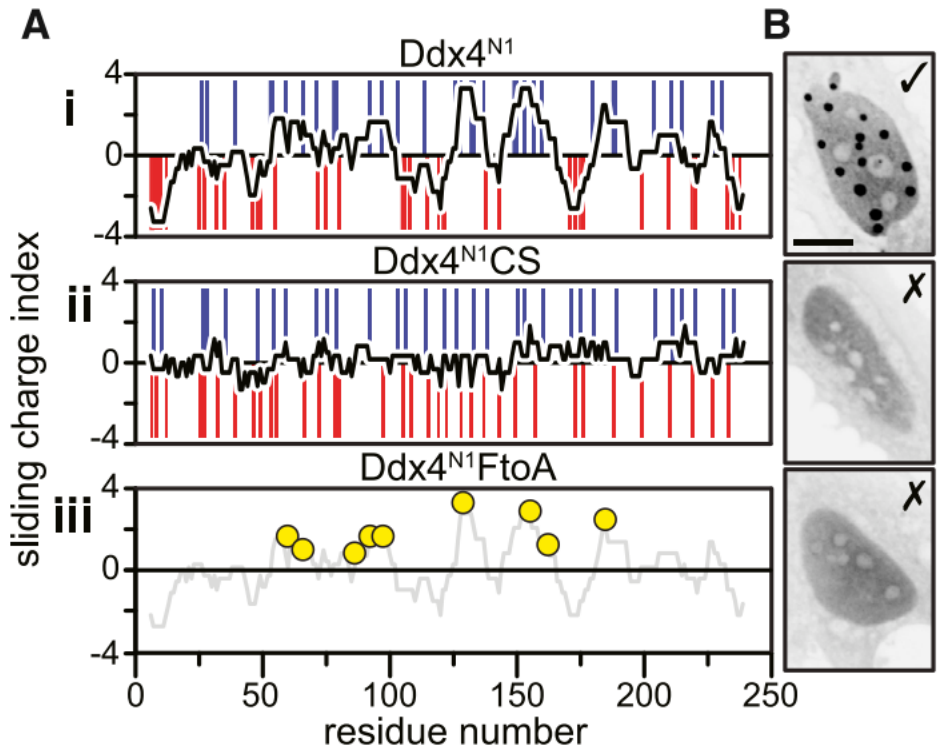

Figure 6: Electrostatic charge blocks facilitate formation of biomolecular condensates.(A) Sliding net charge (10 amino acid window, black) is shown for (i) Ddx4N1 and (ii) a charge-scrambled mutant, Ddx4N1CS, obtained by swapping the positions of positive residues (blue bars) and negative residues (red bars) to minimize any persistence of blocks of charge. (iii) A mutant where nine phenylalanine residues, whose placement was highly conserved, were mutated to alanine, Ddx4N1FtoA. The positions of the nine phenylalanine residues (yellow circles) mutated to alanine are indicated. (B) Representative fluorescence images from cell imaging experiments reveal that Ddx4N1CS and

Ddx4N1FtoA do not form organelles in cells under physiological conditions. Residual HeLa nucleoli are still observed as fluorescence-depleted regions within the cell nucleus. Adapted from Nott, T. J. et al. (2015). Phase Transition of a Disordered Nuage Protein Generates Environmentally Responsive Membraneless Organelles. Molecular Cell, 57(5), 936–947.

1.6 Protein Localization in Bacteria

While researchers now understand the prevalence of biomolecular condensates and some mechanistic details of their formation, Oparin's original conception of phase-separating, condensate structures were not eukaryotes—they were simpler even than modern prokaryotes. To embrace the possibility of his predictions of phase separation as central to the origin of life, it is necessary to follow the evolutionary trail back in time through more primitive, bacterial organisms. Any biomolecular condensates found in bacteria might help elucidate the condensate features shared by ancestral phase-separating organisms.

Until recently, however, the idea of any form of organization in bacterial cells was surprising. Early observers of bacterial cells noticed that these prokaryotes did not possess the membrane-bound compartments by which eukaryotes organize so much of their cellular biochemistry[20,21] This lack of membranous, walled architecture does not preclude internal organization in bacterial cells, as early investigations of *E. coli* and *C. crescentus* demonstrated.[22,23] Subcellular localization of the FtsZ cell division ring to the midcell in *E. coli* and of the MCP chemoreceptor to the cell pole in *C. crescentus* and *E. coli* is essential for proper function of both structures.[22,23] And these early investigations were not anomalies—in *C. crescentus* more than ten percent of the proteome displays subcellular localization, equivalent to roughly 300 proteins.[24]

Without membranous compartments to dictate subcellular localization, how are these bacterial proteins guided to their niche? The simplest mechanism is diffusion and capture, in which a protein localizes via interaction with another protein already found at its destination (Figure 7A).[21] Large hub proteins like DivIVA in *B. subtilis* are able to recruit and localize many other proteins to their positions at the cell pole, but ultimately the hub protein itself somehow recognizes its position at the pole so it can serve as this anchor.[21,25]

For proteins at the pole—essential to many cellular processes in bacteria—there are three main mechanisms for localization. One technique, used by the hub protein DivIVA, is recognition of the highly curved surface of the membrane at the cell pole. Through oligomerization and assembly into a large structure, DivIVA is able to sense membrane curvature and assembles at these locations via stabilizing interactions with the membrane (Figure 7B).[21,26] A second mechanism of localization to the cell pole is also mediated by oligomerization, as exemplified by the PopZ protein in *C. crescentus*. Although this protein does not recognize curvature, it self-associates to assemble into a large polymer. This aggregate is pushed towards the poles of the cell because it is excluded from the densely packed nucleoid of chromosomal material occupying the midcell (Figure 7C, Figure 8).[21,27,28] Finally, other proteins are targeted to the polar region via interaction with pole-specific features (Figure 7D). The phospholipid cardiolipin preferentially localizes to the polar region due to its cone shape, and proteins interacting with it are thus enriched at the poles.[21] Researchers also hypothesize that proteins may interact specifically with the aged peptidoglycan at the poles—most new synthesis occurs at the sidewall—though this form of localization has not been proposed often.[21]

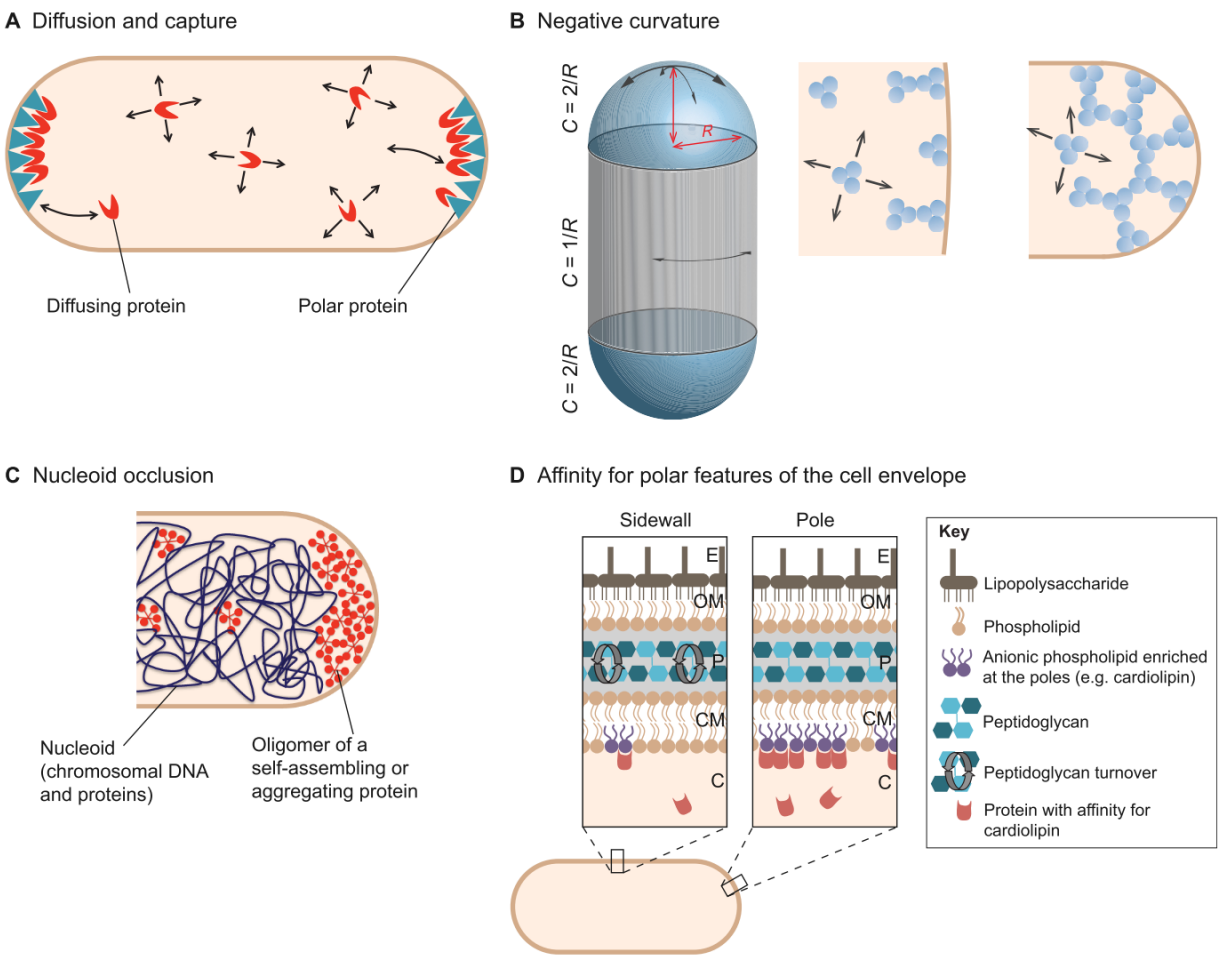

Figure 7: Mechanisms of polar protein localization in bacteria (A) A protein (e.g. ParA1 in V. cholerae) diffusing in the cytoplasm (as indicated by single arrows) is trapped at the poles transiently (double arrows) through an affinity for a polar protein (e.g. HubP in V. cholerae) that is already localized at the cell poles. (B) Higher-order protein assemblies are favored in membrane regions of stronger curvature. Left: representation of a rod-shaped cell showing the radius of curvature (R) and the stronger negative curvature (C, curved arrows) at the cell poles (blue areas) compared with the sides of the cylinder (gray area), as described previously (Huang and Ramamurthi, 2010). Middle and right: formation of a higher-order protein assembly occurring preferentially in membrane regions of stronger negative curvature (e.g. DivIVA in B. subtilis). Arrows indicate the free diffusion of oligomers. (C) Formation of large protein assemblies such as higher-order structures (e.g. PopZ in C. crescentus) or protein aggregates (e.g. misfolded proteins in *E. coli*) is energetically favored outside the nucleoid region. (D) Differences in composition of the cytoplasmic membrane and peptidoglycan between cell poles and the rest of the cell envelope can serve as cues for localization of polar proteins. The particular case of a protein (e.g. ProP in *E. coli*) that preferentially binds anionic

phospholipids enriched at the poles, such as cardiolipin, is depicted. E, extracellular space; OM, outer membrane; P, periplasmic space; CM, cytoplasmic membrane; C, cytoplasm. Note that the schematics in all figures are not to scale and do not reflect the structure of the illustrated proteins. Reproduced with permission from The Company of Biologists, Laloux, G., & Jacobs-Wagner, C. (2014). How do bacteria localize proteins to the cell pole? Journal of Cell Science, 127(1), 11–19.

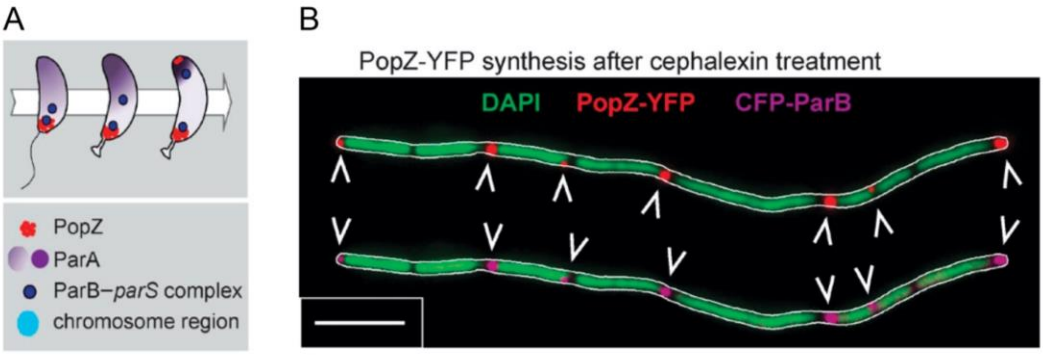

Figure 8: PopZ polar localization by nucleoid occlusion (A) PopZ localization throughout the cell cycle in C. crescentus. Multimerization favors the established matrix at the old pole until a new, nucleoid free region is created through cell elongation and the accumulation of PopZ binding partner ParA favors establisment of a new polar matrix. (B) *E. coli* cells were treated with cephalexin for 2 h before induction of PopZ-YFP and CFP-ParB synthesis for 1 h. The nucleoid region of cells was stained with DAPI before imaging (scale bar is 5 μm). Overlays of DAPI and PopZ-YFP (top) or CFP- ParB (bottom) with the MicrobeTracker cell outline are shown. Arrowheads indicate polar and nonpolar foci. PopZ accumulates in non-nucleoid regions of the pole and the cell body, and accumulation of CFP-ParB in the PopZ foci demonstrates that PopZ foci retain functionality. The ability of PopZ to form polar foci when expressed heterologously in *E. coli* indicates its functional independence from polar landmark proteins in its native C. crescentus, and demonstrates the power of multimerization and nucleoid occlusion alone to dictate polar.localization Adapted with permission from Rockefeller University Press, Laloux, G., & Jacobs-Wagner, C. (2013). Spatiotemporal control of PopZ localization through cell cycle-coupled multimerization. Journal of Cell Biology, 201(6), 827–841.

1.7 Biomolecular Condensates in Bacteria—BR Bodies

A recent investigation into the most common bacterial mRNA processing protein, called RNase E, added a new mechanism of subcellular organization to the bacterial arsenal, revealing that bacteria can also use phase separated biomolecular condensates to organize their contents.[29] The RNase E protein performs an incredibly similar function to the first biomolecular condensate that Clifford Brangwynne discovered in *C. elegans* a decade earlier. That condensate, the p granule, selectively degrades mRNA transcripts to guide *C. elegans* embryogenesis, and RNase E assembles a complex of catalytic proteins that degrade mRNA transcripts in response to stress conditions.[13,29]

In addition to performing functions similar to eukaryotic biomolecular condensates, RNAse E displays many of the hallmark features of phase-separating proteins. Like the proteins found in eukaryotic neuronal granules that Kato et al. studied, RNAse E phase separates via an intrinsically disordered region.[16,29] This region forms multivalent interactions—its mechanism of phase separation—with both other copies of the RNAse E protein and with mRNA transcripts through positively and negatively charged patches of amino acids, as do many eukaryotic phase separating proteins.[18,29] Finally, like the p granule biomolecular condensate in *C. elegans*, RNAse E phase-separated droplets fuse together over time in the cell to create larger, spherical liquid droplets.[13,29]

This discovery shows that bacteria, as well as eukaryotes, use a mechanism similar to the one Oparin predicted to create internal organization—and these bacterial condensates may represent a more ancient, closer link to the coacervates Oparin predicted than those relatives found in eukaryotic cells.

In the few years since the discovery of RNAse E's status as the first prokaryotic biomolecular condensate, many other bacterial proteins have been shown to act as condensates. Though the overall number of disordered regions in bacterial proteins is low—only 2-5% of the proteome—those proteins that do contain disorder and act as biomolecular condensates participate in key functions of the bacterial cell cycle.[30]

One function where condensation plays a key role is in transcription, where RNA polymerase (RNAP) forms clusters in *E. coli* during log phase growth and division.[31] Ladouceur et al. found that this clustering occurs with the assistance of an antitermination factor protein called NusA (Figure 9A).[31] This protein contains six folded domains connected by flexible linker regions, with each folded domain able to interact with other proteins involved in transcription—a classic example of the multivalent interactions characteristic of biomolecular condensation.[18,31] Furthermore, Ladouceur et al. observed NusA forming liquid liquid phase separated droplets *in vitro*, under crowded physiological conditions imitated by introducing dextran (Figure 9B, C).[31] In conjunction with single molecule tracking observations showing that diffusion of transcription proteins in RNAP clusters is slowed compared to the cytoplasm, but faster than diffusion of proteins bound to the nucleoid, Ladouceur et al. concluded that RNAP and associated transcription proteins cluster in phase-separated liquid condensates during growth conditions in which transcriptional efficiency is needed.[30,31]

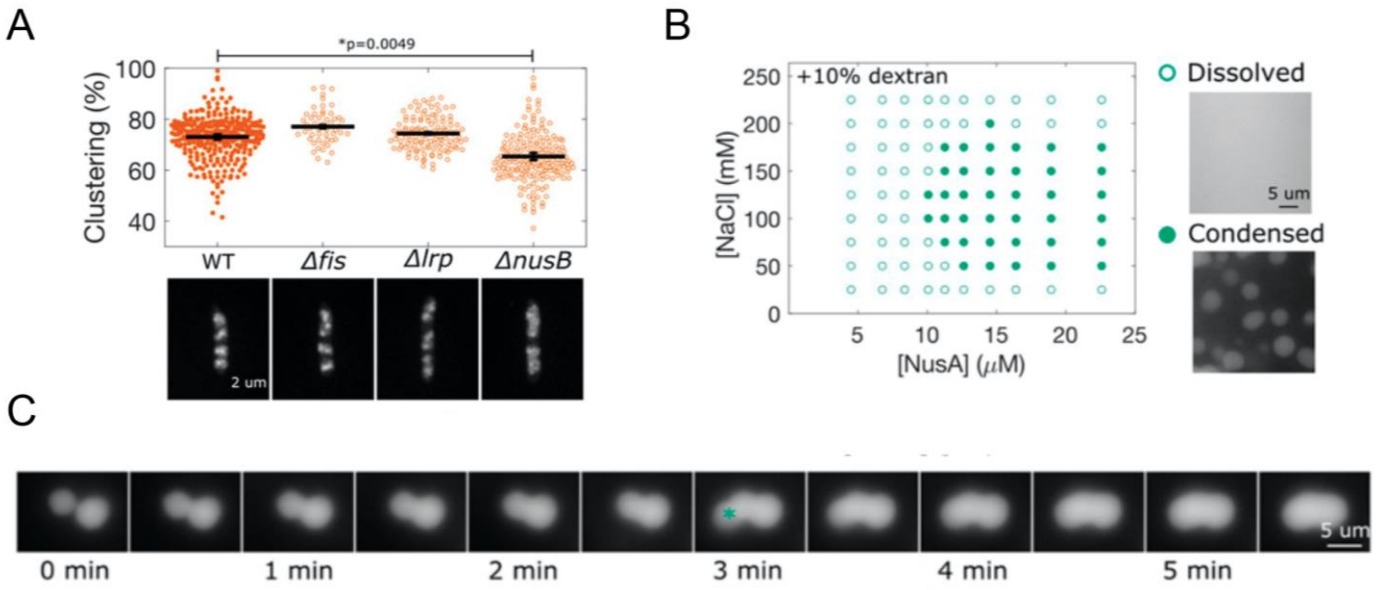

Figure 9: Bacterial transcription protein NusA forms RNA polymerase-containing biomolecular condensates in *E. coli* (A) Clustering and fluorescence images of WT and deletion mutants expressing the RNA polymerase (RNAP) subunit RpoC tagged with mCherry. Proteins tested for RNAP cluster formation include fis—a disordered transcription factor expressed at the same time as RNAP—and NusB, an antitermination factor that colocalizes to RNAP clusters with NusA (which is essential in *E. coli*). P values were calculated by ANOVA and Tukey–Kramer post hoc test. Removal of NusB—and by extension, interruption of the antitermination complex containing NusA—disrupted RNAP cluster formation. (B) Phase diagram for purified NusA in the presence of 10% dextran. Open circles indicate conditions in which the protein is dissolved; closed circles indicate conditions in which the protein is condensed, forming condensates. (C) Montage of NusA droplet fusion indicating liquid behavior. A third droplet falls from solution at t = 3 min (marked by *). Adapted from Ladouceur, A. M. et al. (2020). Clusters of bacterial RNA polymerase are biomolecular condensates that assemble through liquid-liquid phase separation. Proceedings of the National Academy of Sciences of the United States of America, 117(31), 18540–18549. Copyright 2020 National Academy of Sciences.

Another important bacterial function involving biomolecular condensates is the ParABS system in *E. coli*. This complex of proteins is responsible for the initial steps in segregation of each

copy of the bacterial chromosome to the poles of the cell during cell division.[32] Guilhas et al. demonstrated that ParB proteins form condensates nucleated by the ParS DNA sequence located near the origin of replication.[32,33] These condensates are highly condensed liquid clusters of ParB dimers clustered on and around the ParS region of the chromosome, and Guilhas et al. observed these condensate clusters fusing with one another and exchanging dimers of ParB when they were photobleached and allowed to recover.[33] Interestingly, fusion of individual ParB condensates does not occur at long time scales, as would be expected if liquid condensates are unrestricted. Guilhas et al. found that the ParA ATPase—involved in movement of the origin to the pole of the cell—restricts fusion of ParB condensates, and that this restriction depends on the ATPase activity of ParA.[33] This points to a potential wider mechanism of the localization of bacterial condensates within the cell by motor proteins.

1.8 PopZ as a Bacterial Biomolecular Condensate

A particularly interesting bacterial condensate is the *C. crescentus* protein PopZ.[30] *Caulobacter crescentus* has been a focus of study because it divides asymmetrically into two cell types which are both morphologically and physiologically distinct—an immobile stalked cell capable of reproduction and a mobile swarmer cell incapable of division until it differentiates into the stalked form.[34] The pole organizing protein PopZ (for pole-organizing protein that affects FtsZ), acts as a hub coordinating many of the processes necessary to generate this asymmetric division, from chromosome segregation to positioning cell division machinery to interacting with key cell cycle signaling proteins.[35]

Recently, Lasker et at. demonstrated that PopZ's functions as a biomolecular condensate are critical to forming the gradient of the phosphorylated transcription factor CtrA-P that dictates *C. crescentus* asymmetric division. As a condensate, PopZ forms a microdomain at each cell pole and selectively admits certain binding partners—in this case the membrane associated kinase/phosphatase CckA, the phosphotransferase ChpT, and the transcription factor CtrA. Concentration of CckA by PopZ at the new cell pole stimulates its kinase activity, and the close proximity of ChpT bound to PopZ and CtrA bound to ChpT enable transfer of the phosphate group through ChpT to CtrA (Figure 10). Phosphorylated CtrA slowly diffuses out of the PopZ condensate at the new pole, and the gradient of CtrA-P established by this process dictates that the new pole progeny cell takes on the swarmer form after division and the old pole progeny remains stalked after division.[36] The selective admission of binding partners and reduction of diffusion rates within the branching oligomeric matrix of the PopZ microdomain enable classification of the domain as a biomolecular condensate.[36]

With the presence of phase-separated biomolecular condensates in more primitive prokaryotic bacteria now well established, understanding the potential ancient ancestors of these condensates will be facilitated through further exploration of condensates across different prokaryotic species and comparison of their common features. A way to facilitate understanding of the common or minimal set of components necessary to form a condensate—as well as generate useful tools for biotechnology applications—is to attempt to build *de novo* modular condensates.

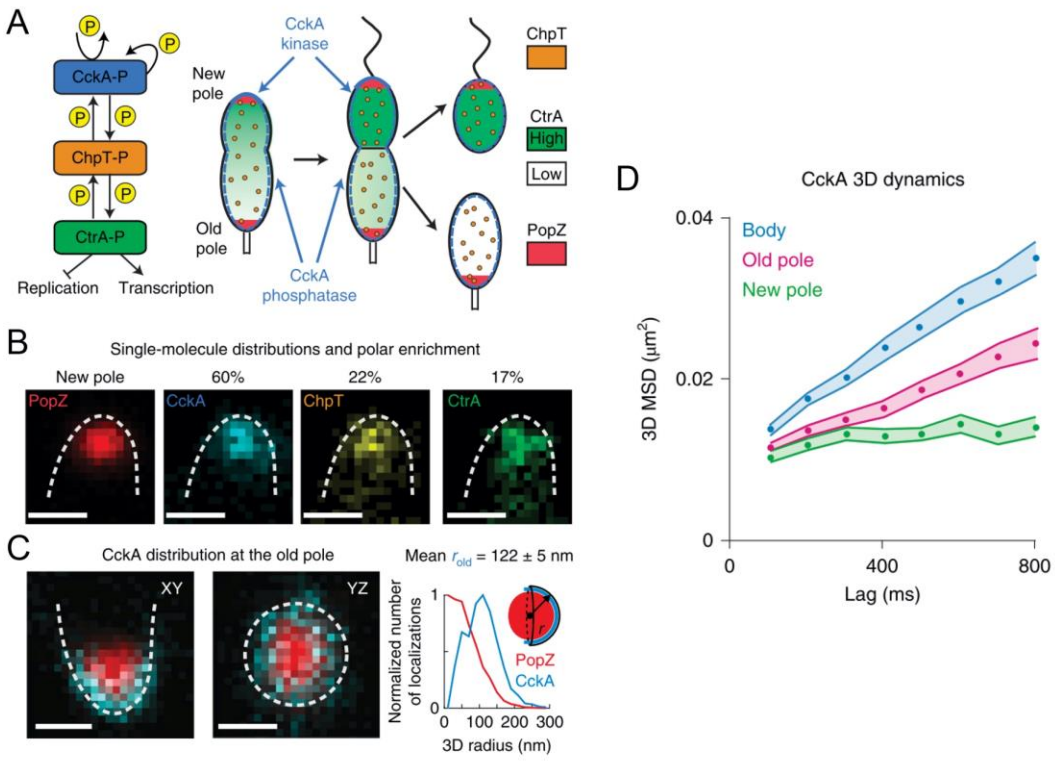

Figure 10: PopZ is a biomolecular condensate critical to asymmetric division in *C. crescentus* Diagram of signal flow and subcellular localization of the CtrA/CckA/ChpT phospho-signalling pathway relative to PopZ. (B) Average single-molecule distributions of PAmCherry-PopZ, CckA-eYFP, ChpT-eYFP and CtrA-eYFP-14 at the new poles of predivisional cells (n = 27, 13, 27 and 60 poles, respectively) registered within the same coordinates using PopZ as a landmark. Percentage values above the images indicate the fraction at the pole in diffraction-limited images. These images demonstrate concentration of key asymmetric division signaling proteins in the small PopZ microdomain at the new pole. (C) Average CckA and PopZ polar distributions using 3D localization data from n = 29 old poles (2,006 and 5,282 localizations, respectively). Slices (200 nm) are shown to emphasize the radial CckA distribution on the membrane. Plot: radial distribution of CckA and PopZ from the PopZ centroid with volume-normalized density (error bars, 95% confidence interval of resampled localizations). A similar analysis was not done with PopZ and CckA at the new pole due to the new pole's smaller size. (D) 3D MSD curves for CckA tracks within selected cellular regions. CckA diffuses more quickly in the larger volume of the PopZ microdomain at the old pole than it does in the smaller PopZ microdomain at the new pole, with this difference in concentration likely responsible for kinase activity—initiated by autophosphorylation in close quarters—observed at the new pole and the phosphatase activity in the more spread out old pole. Differential kinase/phosphatase activity of CckA in the new vs old poles is responsible for the

downstream signaling cascade leading to asymmetric cell division in *C. crescentus.* Figure adapted by permission from Springer Nature: Lasker, K. et al. (2020). Selective sequestration of signalling proteins in a membraneless organelle reinforces the spatial regulation of asymmetry in Caulobacter crescentus. Nature Microbiology, 5(3), 418–429.

1.9 *De Novo* Biomolecular Condensates in Bacteria

Recently, several different strategies for *de novo* construction of liquid, phase-separated condensates have been attempted. One draws on earlier observations in eukaryotes that charged regions facilitate liquid-liquid phase separation, and uses supercharged GFP to create synthetic biomolecular condensates in *E. coli*.[18,37] Operating under the assumption that the positively charged GFP mutants they created would phase separate with endogenous, negatively charged RNA, Yeong et al. tested GFP mutants ranging from +6 to +36 in surface charge, and they found that constructs from +12 up to +36 formed compartments in *E. coli*.[37] These compartments were liquid, phase-separated condensates, they concluded, because fluorescence recovery after photobleaching (FRAP) experiments indicated that the GFP-formed compartments exchanged more rapidly than a GFP mutant forming inclusion bodies.[37] Lastly, they confirmed that these compartments did include RNA—as predicted—and excluded DNA.[37]

Another strategy, from the Lindner group, is constructing *de novo* phase-separating condensates entirely from RNA. They created phase-separating RNA molecules by fusing 47 repeats of the CAG triple-ribonucleotide repeat sequence (rCAG)—known to cause liquid-like puncta in human cells—to 12 repeats of the MS2 RNA aptamer sequence that binds the MS2 coat protein.[38] The group called these constructs Transcriptionally Engineered Addressable RNA Solvent droplets (TEARS), and found that the TEARS were able to exclude endogenous proteins

that were not addressed to the condensate via aptamer binding.[38] They then demonstrated that RNA molecules targeted to these condensates were exhibited slowed transcription, and that biosynthetic pathway member enzymes could be targeted en mass to the TEARS for enhancement of synthesis or individually to interrupt production.[38]

Along with efforts to construct fully synthetic condensates, researchers are beginning to utilize native condensates in synthetic biological systems. In particular, the wide-ranging utility of PopZ in organizing diverse cellular processes and facilitating asymmetric division in *C. crescentus* make it an attractive condensate to utilize in synthetic biology. Last year, researchers used PopZ as part of systems designed for purposes ranging from investigating protein interactions to generating asymmetric cell division in *E. coli*.[39–41]

Lim and Bernhardt took advantage of PopZ's selective admittance of binding partners to create a two-hybrid assay for non-cytoplasmic proteins in *E. coli*.[41] By fusing the H3H4 homo-oligomerization domain—used by PopZ for polymeric clustering—and GFP to their bait protein of choice, they were able to localize the bait to a single pole in *E. coli*. They then observed their prey construct—fused to mScarlet—to see if it colocalized with the PopZ bound prey (Figure 11). By adding transmembrane domains and secretion signal sequences to the bait and prey where appropriate, Lim and Bernhardt were able to use this system to observe interactions between inner membrane and cytosolic proteins, between two inner membrane proteins, between inner membrane and periplasmic proteins, and even interactions between inner and outer membrane proteins.[41]

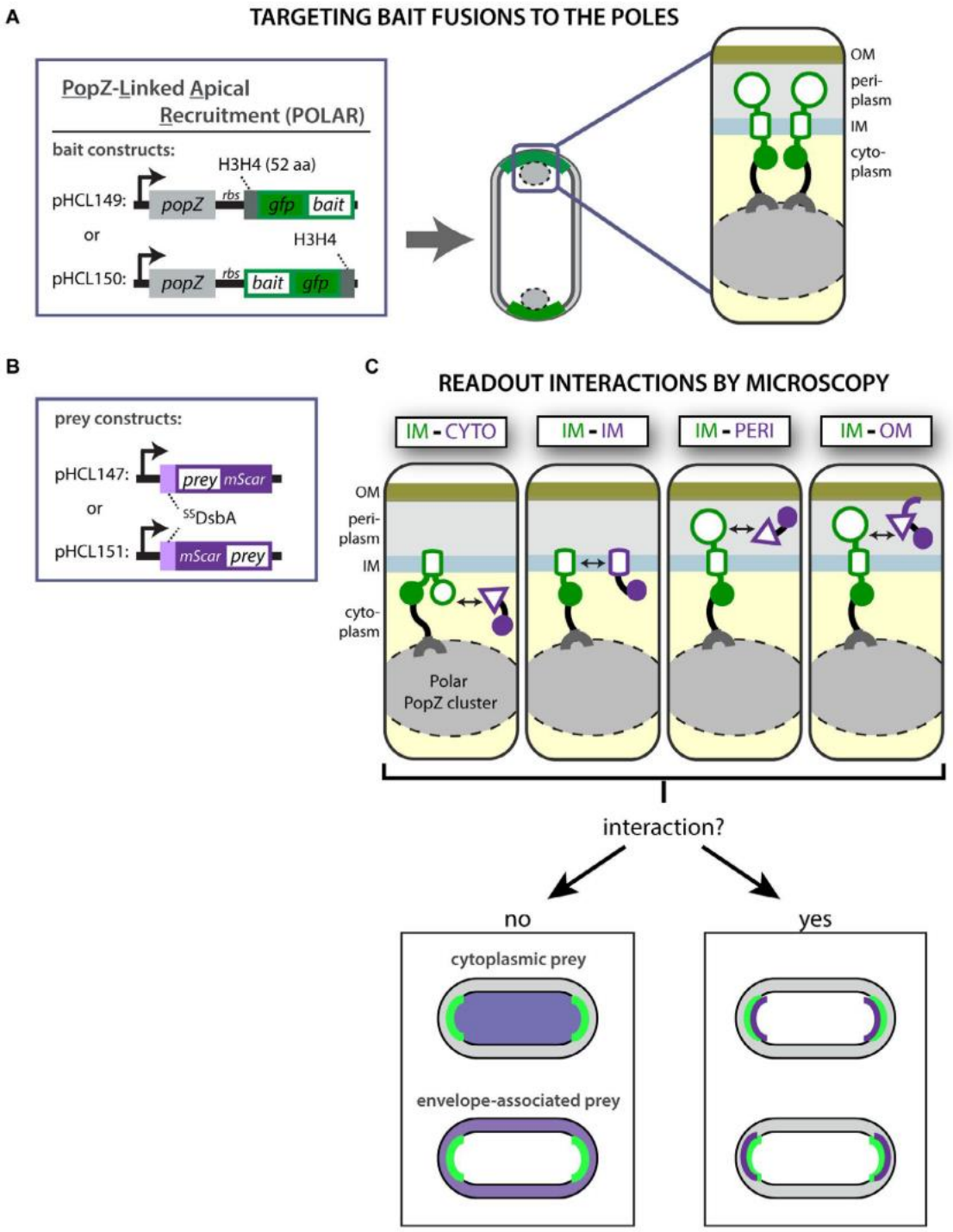

Figure 11: Using PopZ as a tool in synthetic biology—the POLAR protein interaction assay (A) The POLAR assay takes advantage of PopZ from *C. crescentus*, which spontaneously forms clusters at the cell poles of *E. coli*. Shown are expression plasmids for the production of unlabeled PopZ along with GFP fusions to the bait protein of choice. The fusion also includes a H3H4 peptide of PopZ that is sufficient to recruit the labeled bait protein to PopZ

polar clusters. (B) Shown are expression plasmids for the production of mScar fusions to the prey protein of choice. SSDsbA indicates the signal sequence of DsbA of *E. coli*, which is utilized to facilitate efficient secretion to the periplasmic space. Note that the signal peptide is cleaved upon secretion. (C) The POLAR assay can be used to assess interactions of cytoplasmic and exported prey proteins with a membrane-embedded bait. The fusion of the prey and the bait to mScar and GFP, respectively, enables assessment of interaction by fluorescence microscopy. A positive interaction results in the recruitment of a prey to the cell pole by the polarly localized bait. Reprinted by permission from John Wiley and Sons, Lim, H. C., & Bernhardt, T. G. (2019). A PopZ-linked apical recruitment assay for studying protein–protein interactions in the bacterial cell envelope. Molecular Microbiology, 112(6), 1757–1768.

Even more ambitious than protein interaction assays are two groups who used PopZ to create synthetic asymmetric cell division in *E. coli*.[39,40] As a primary player in the pathway responsible for the morphologically dramatic asymmetry of division in *C. crescentus*, PopZ is also a good choice for creating asymmetry in *E. coli* because it localizes to the just the old pole when *E. coli* divides.[42] Grant Bowman's group utilized this single-pole property to define a physical cue for asymmetric division, and then recruited a phosphodiesterase (PDE) enzyme to PopZ.[39] In the strain with a pole-localized PDE, they also expressed a cytosolic diguanylate cyclase (DGC), thus setting up a system in which cyclic-di-GMP is broken down at the old pole and synthesized in the cytoplasm (Figure 12). Upon division, then, the daughter cell inheriting the PopZ condensate and its recruited PDE had a low concentration of c-di-GMP while the other daughter cell had a high concentration of c-di-GMP. The group was then able to link differences in c-di-GMP concentration to differential gene expression between daughter cell types.[39]

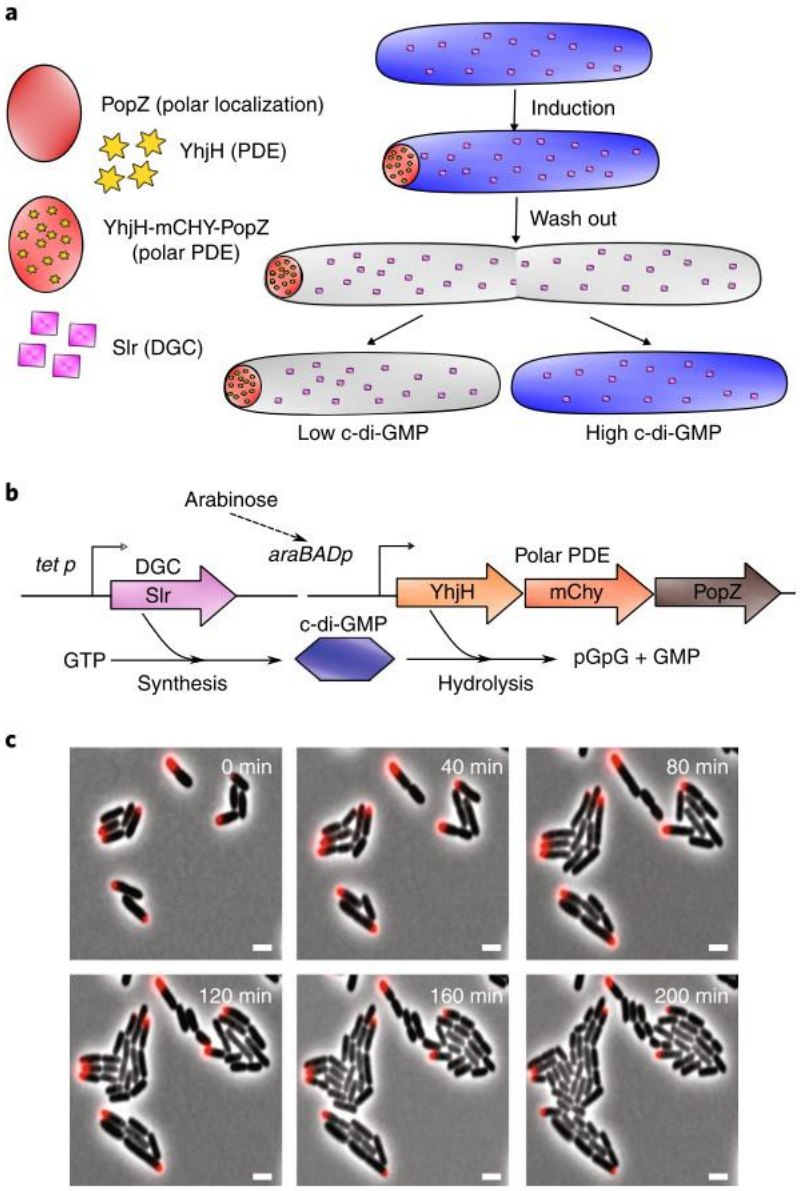

Figure 12: Using PopZ to engineer synthetic asymmetric cell division in *E. coli* (A) PopZ, which forms a macromolecular structure that becomes localized to *E. coli* cell poles, is part of a tripartite fusion protein that includes a phosphodiesterase (PDE) and a mChy tag. A DGC is expressed at low levels and distributed throughout the cytoplasm. After transient expression of the PopZ fusion protein, the next cell division is asymmetric with respect to the inheritance of PopZ and the accumulation of c-di- GMP levels via PDE and DGC activities. (B) A genetic circuit for generating asymmetric cell division with respect to c-di-GMP signaling. (C) Observation of polar asymmetry and asymmetric cell division. In cells bearing plasmid pBad-YmP, YhjH-mChy-PopZ expression was induced with arabinose for 2 h, washed to remove the inducer, then mounted on an agarose pad for observation of growth and

division by time-lapse fluorescent microscopy. Three independent trials produced similar results. Scale bars, 2 μm. Reprinted by permission from Springer Nature, Mushnikov, N. V. et al. (2019). Inducible asymmetric cell division and cell differentiation in a bacterium. Nature Chemical Biology, 15(9), 925–931.

Matthew Bennett's group also used PopZ as a base upon which to build asymmetric cell division in *E. coli*.[40] They borrowed elements of the *C. crescentus* chromosomal partitioning system—not found in *E. coli*—and used it with PopZ to partition plasmids asymmetrically at division. By placing the ParS DNA sequence on one plasmid and the ParB protein encoding sequence on another, Bennett's group created a strain where the ParB protein bound the ParS sequence and clustered all copies of the PasS-containing plasmid to one pole. These clustered plasmids were then segregated into one daughter cell upon division because ParB binds to old-pole-localized PopZ. By adding motility genes to the segregated plasmid, the group was able to create a system in which one daughter cell was motile and the other sessile.[40]

Thus, it is clear that work is underway to better understand biomolecular condensates in bacteria by creating synthetic condensates and to use native condensates to achieve greater control over biosynthesis in bacteria. Now, we attempt to bridge those two goals by using PopZ as a model from which to construct fully synthetic condensates in *E. coli* which are capable of the same biosynthetic functions as PopZ. Our synthetic constructs should be capable of forming a physical landmark for asymmetric cell division in *E. coli* and of recruiting partner enzymes to biochemically and transcriptionally produce asymmetry in daughter cells. Along the way, we hope these synthetic scaffolds will provide clues about the characteristics shared by the primordial, phase-separated coacervates Oparin described.

2.0 Design of Synthetic Condensates Based on Peptide Hydrogels

2.1 Introduction

2.1.1 Synthetic Condensate Design Inspiration

In this study we sought to create a simple synthetic condensate capable of acting as membraneless organelle for customized functions such as the regulation of gene expression. As a second goal, we aimed to understand if and how synthetic condensates could selectively accumulate at one cell pole as this will provide a foundation for asymmetric cell division. We drew inspiration from PopZ, a self-assembling cell-pole hub protein in the α-proteobacterium *Caulobacter crescentus.* We were also drawn to the similarities in domain architecture between PopZ and the simpler *de novo* peptide hydrogels designed for biomedical applications by the Tirrell Lab.[39,42,43]

In *C. crescentus,* PopZ functions as a polar hub that binds signaling proteins key to asymmetric cell division into swarmer and stalked daughter cells.[36,44] These include the transmembrane histidine kinase CckA and the cytoplasmic phosphotransferase ChpT, which together provide the only phosphate source for the cell-fate determining transcription factor CtrA.[36] At the new pole, concentration of CckA by PopZ stimulates its kinase activity, and the close proximity of ChpT bound to PopZ and CtrA bound to ChpT enable transfer of the phosphate group through ChpT to CtrA (Figure 13).[36] Meanwhile, at the old pole, CckA is less concentrated by PopZ and behaves as a phosphatase (Figure 13).[36] The slow diffusion of CtrA away from PopZ at the new and old poles in its respective phosphorylated or dephosphorylated state creates a

concentration gradient of CtrA-P, with greater amounts of phosphorylated CtrA at the new pole activating a gene transcription program that creates a swarmer daughter cell and greater amounts of dephosphorylated CtrA at the old pole inhibiting replication and resulting in a stalked daughter cell (Figure 13).[36]

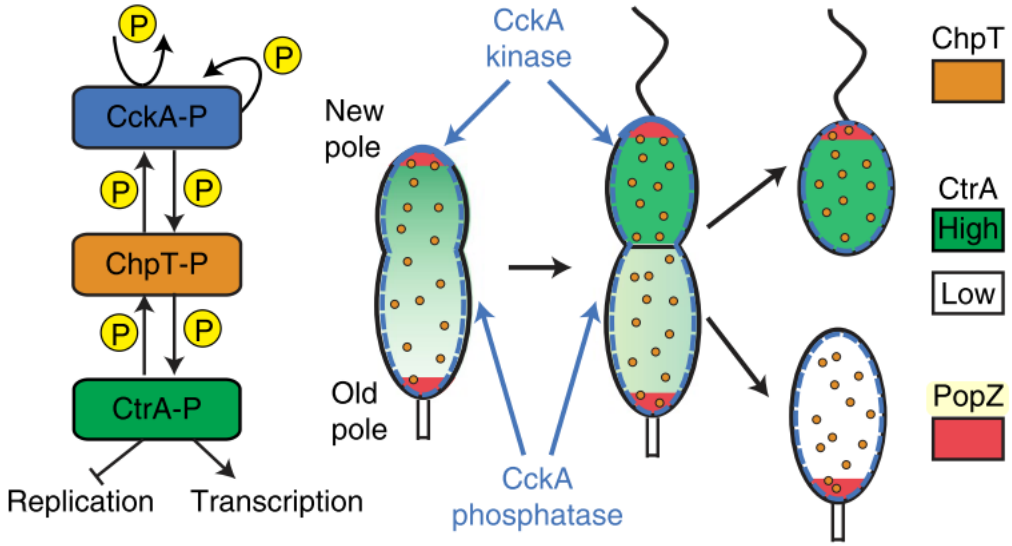

Figure 13: *C. crescentus* asymmetric division signaling controlled by PopZ Diagram of signal flow and subcellular localization of the CtrA/CckA/ChpT phospho-signalling pathway relative to PopZ. Figure adapted by permission from Springer Nature: Lasker, K. et al. (2020). Selective sequestration of signalling proteins in a membraneless organelle reinforces the spatial regulation of asymmetry in Caulobacter crescentus. Nature Microbiology, 5(3), 418–429

PopZ slows the diffusion of CtrA by assembling into a biomolecular condensate at the poles in *C. crescentus.* The Bowman group demonstrated that PopZ diffuses through the cytoplasm more quickly than does the aggregate-forming protein IscA, but more slowly than freely diffusing GFP.[44] Later, the Shapiro group found that the diffusion of binding partner CckA is slowed two to fourfold in the PopZ foci at the pole compared to its diffusion in the cell body.[36] Both of these lines of evidence point towards phase separation behavior indicative of biomolecular condensates.[18] However, it's unclear if the PopZ biomolecular condensates exhibit liquid-like

properties or more solid-like properties similar to a hydrogel. Nevertheless, PopZ forms functional micron-sized "organelle-like" assemblies that regulate signal transduction in bacteria.

The structure of PopZ enables its condensate assembly and its ability to bind partner signaling proteins. PopZ is composed of a central disordered region flanked by helical regions at its N- and C-termini.[45] The central region of PopZ contains a negatively-charged, intrinsically disordered section called the PED region. This area, together with the N-terminal helix H1 and the C-terminal helix H2 are responsible for binding the many cell cycle regulatory proteins, including CckA and ChpT, which PopZ localizes to the cell pole (Figure 14A).[44,45] The remainder of the C-terminal region, composed of two alpha helices called H3 and H4, is responsible for oligomerization of PopZ into hexamers, which then assemble end-to-end to form higher-order oligomeric structures (Figure 14A, B).[44,45]

While the C-terminal H3 and H4 helices are responsible for oligomerization and formation of higher order structures, the protein-binding region of PopZ is necessary for proper localization of PopZ condensates in *C. crescentus.*[28] Through the swarmer phase of the *C. crescentus* life cycle, PopZ is present only at the old pole.[27,42] As replication is initiated, PopZ undergoes a unipolar to bipolar transition facilitated by binding to the ParA protein (Figure 15A).[28] ParA concentration increases at the new pole region during replication, and PopZ bound to ParA at the new pole nucleates formation of a second condensate, made favorable also by the absence of the chromosome at this second polar region (Figure 15B).[28] Removal of the part of the PopZ binding region that associates with ParA—the N terminal section containing helix H1—prevents the transition from unipolar to bipolar localization of PopZ (Figure 15C).[28]

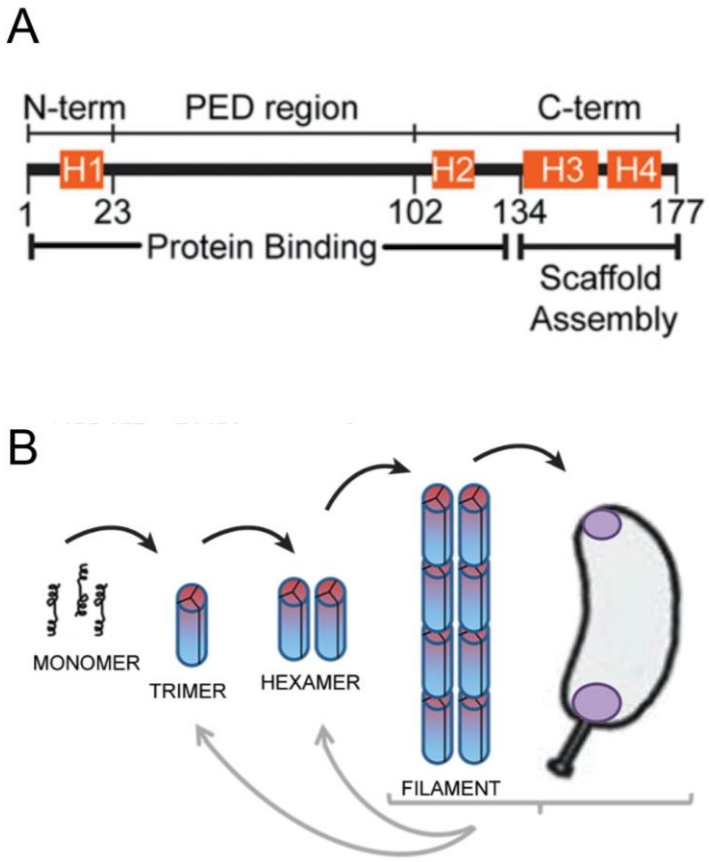

Figure 14: PopZ domain structure and higher order assembly (A) Functional regions in the primary sequence of PopZ. (B) A model showing the relationship between PopZ assembly and sub-cellular localization. The first step is the self-association of monomers into rod-shaped trimers, which subsequently dimerize through lateral contact to form hexamers. End-to-end contacts between hexamers produce filaments, and in vivo, these filaments accumulate at cell poles. Each step in this process can be blocked by a mutation in PopZ, as indicated. Each of the forms is metastable and its frequency is influenced by protein concentration and conditions in the buffer or cell extract. Adapted with permission from Rockefeller University Press, Laloux, G., & Jacobs-Wagner, C. (2013). Spatiotemporal control of PopZ localization through cell cycle-coupled multimerization. Journal of Cell Biology, 201(6), 827–841 and from Holmes, J. A. et al. (2016). Caulobacter PopZ forms an intrinsically disordered hub in organizing bacterial cell poles. *Proceedings of the National Academy of Sciences*, *113*(44), 12490–12495

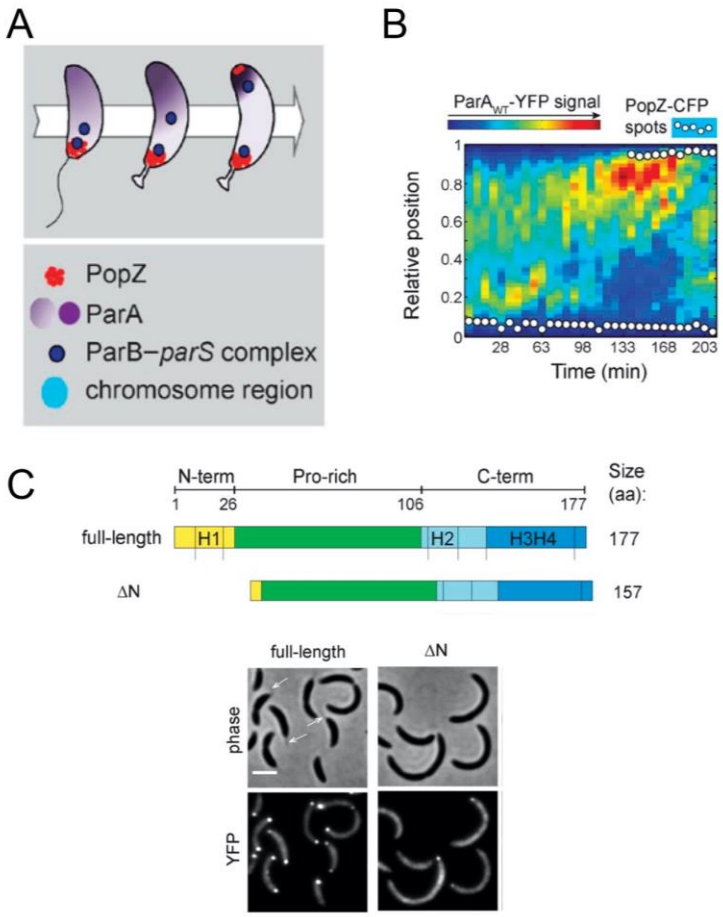

Figure 15: PopZ polar localization in *C. crescentus* (A) Unipolar to bipolar transition of PopZ: Accumulation of the protein partner (ParA) results in a local increase in the concentration of diffusing self-assembling proteins (PopZ oligomers) to a level that promotes and sustains assembly into a higher-order structure (PopZ matrix) where and when the cell cycle event takes place. In the case of PopZ, a coupling with the ParA-dependent segregation of ParB–parS allows for the controlled assembly of a PopZ matrix at the new pole in time to capture the partitioning ParB–parS complex. (B) Swarmer C. crescentus cells producing $ParA_{K20R}$ (ParA mutant K20R expressed here stalls the ParB/*parS* complex so that only $ParA_{wt}$ is found at the new cell pole where we see PopZ accumulating) were imaged every 7 min. The kymograph of the ParA-YFP signal is shown for a representative cell, along with the relative position of the PopZ-CFP foci (white circles). (C) Synthesis of the PopZ-YFP variants was induced for 5 h before imaging. The YFP signal has been scaled for display. Arrows point at stalks. Adapted with permission from Rockefeller University Press, Laloux, G., & Jacobs-Wagner, C. (2013). Spatiotemporal control of PopZ localization through cell cycle-coupled multimerization. Journal of Cell Biology, 201(6), 827–841.

When PopZ is expressed in *E. coli*, on the other hand, it forms a self-assembled condensate at only one cell pole, indicating that PopZ's cell pole accumulation is likely independent of specific *C. crescentus* factors.[27,28,42] This condensate retains properties in *E. coli* that it possesses in *C. crescentus*—exclusion of ribosomes and binding of partners including ParA and CckA—indicating that is still functional in *E. coli*.[28,44] However, its formation at only one pole is stochastic in *E. coli*, with the daughter cell that does not inherit a polar PopZ focus forming a new condensate at either the old pole or the new pole.[27] *E. coli* filamentation experiments with cephalexin in which PopZ foci form in any chromosome-free regions also reinforce the idea that pole-localization in *E. coli* is due to stochastic assembly in open regions of the cytoplasm (Figure 16).[27,28] Without a binding partner at the new pole, like ParA in *C. crescentus*, to force the nucleation of a second polar focus, accumulation of additional PopZ molecules in *E. coli* is confined to the originally nucleated PopZ condensate.

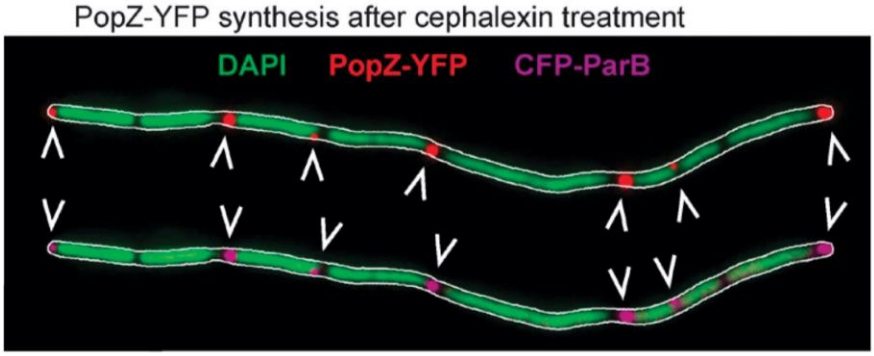

Figure 16: Nucleoid occlusion of PopZ in *E. coli* *E. coli* cells were treated with cephalexin before induction of PopZ-YFP and CFP-ParB synthesis. Cells were stained with DAPI before imaging. Overlays of DAPI and PopZ-YFP (top) or CFP- ParB (bottom) are shown. Arrowheads indicate polar and nonpolar foci. Adapted with permission from Rockefeller University Press, Laloux, G., & Jacobs-Wagner, C. (2013). Spatiotemporal control of PopZ localization through cell cycle-coupled multimerization. Journal of Cell Biology, 201(6), 827–841.

With these observations about PopZ's unipolar assembly in *E.* coli, we noticed a domain structure similar to that of PopZ in the peptide hydrogels designed by the Tirrell group.[43,46] Functionally, the Tirrell group's proteins form gels *in vitro* after expression and purification from *E. coli*, and they intended these gels for use in cell encapsulation and controlled drug release.[43,46] Their gels are formed by synthetic proteins the group calls triblock proteins, with a central disordered 'block' flanked by two alpha-helical 'blocks' (Figure 17).[43,46]

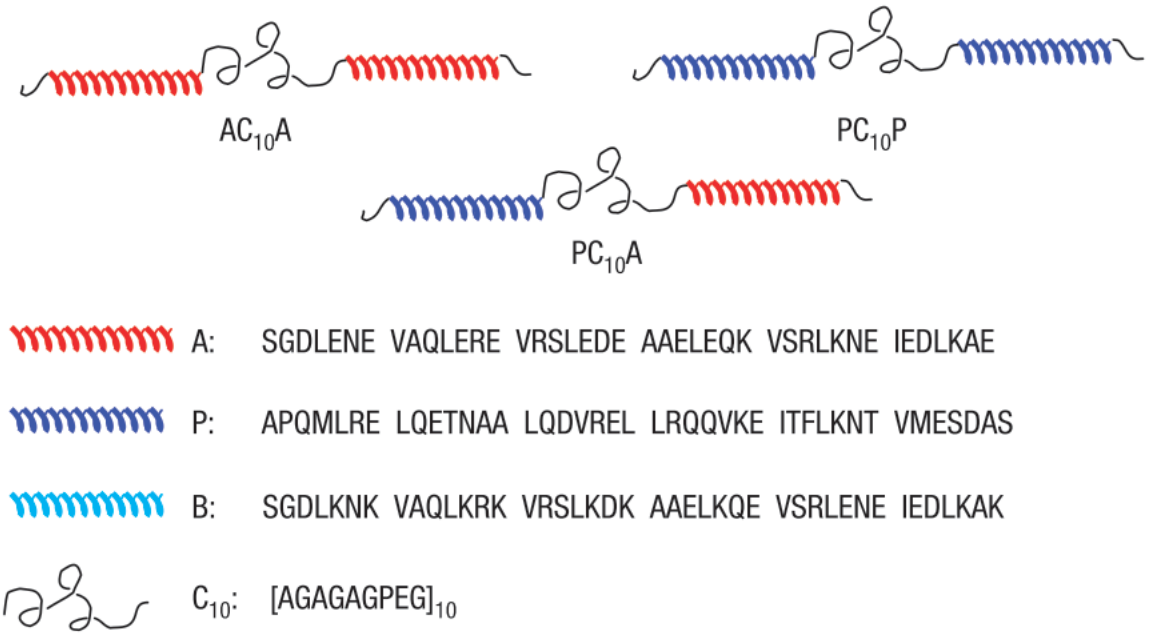

Figure 17: Domain structure of Tirrell hydrogel proteins Protein construct designs and amino acid sequences of several coiled coils (A, P, and B) and the central disordered region (C_{10}) used by the Tirrell group.

The helical 'blocks' the Tirrell group used are leucine zippers.[43,46] These are a subgroup of the larger family of coiled coils, which are alpha helical domains that wind around each other to form a supercoil.[47–49] They are composed of a sequence of seven repeating amino acids, typically referenced a-g, with apolar amino acids at position a and d in the heptad and other positions occupied by polar or charged amino acids (Figure 18A) .[47–49] Positioning hydrophobic amino acids

at positions a and d places them slightly closer together than the periodicity of an alpha-helical turn (averaging one hydrophobic residue every 3.5 residues versus the average alpha helical turn occurring once every 3.6 residues). [47–49] Thus, as coiled coils bind, they supercoil around one another to pack hydrophobic residues into the center of the binding interface (Figure 18 A, B).[47–49] Leucine zippers, such as those the Tirrell group used, have leucine residues as the predominant apolar amino acid at position d.[49]

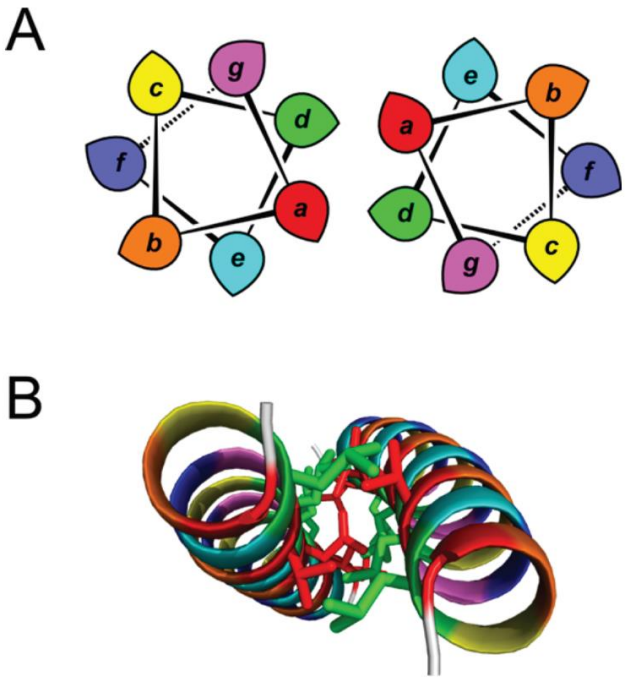

Figure 18: Coiled coil assemblies (A) Helical-wheel diagram showing the heptad repeat configured as a helix with 3.5 residues per turn, i.e., effectively incorporating the supercoil. Leaf shapes indicate the direction of the Cα−Cβ vectors. Hydrophobic residues at the a and d positions provide most of the binding enthalpy, augmented by ion- pairing or hydrogen-bonding interactions between polar residues at opposing e and g positions. The b, c, and f positions are distant from the interface. (B) View down the long axis of a typical parallel, dimeric coiled coil (PDB ID 2ZTA24). Coloring of the heptad positions, abcdefg, follows the CC+ standard for heptad positions (a = red; b = orange; c = yellow; d = green; e = cyan; f = blue; g = magenta).25 Structural images created using PyMol (http://www.pymol.org). Reprinted with permission from Fletcher, J. M. et al. (2012). A basis set of de novo coiled-Coil peptide oligomers for

rational protein design and synthetic biology. ACS Synthetic Biology, 1(6), 240–250.. Copyright 2012 American Chemical Society.

The central region of the Tirrell group's triblock proteins is composed of a polyelectrolyte protein sequence that forms a flexible linker between the two leucine zippers.[43,46] Polyelectrolytes are compounds which, when dissolved in polar solvents (generally water), spontaneously acquire elementary charges distributed along the macromolecular chain.[50] In the case of the Tirrell group's flexible linker, this charge is supplied by glutamic acid residues in the repeated sequence (Figure 17).[43] The charges within this linker ensure that the final oligomerized structure behaves as a gel, including solvent, rather than separating from the solvent to form an aggregate.[46] Circular dichroism analysis of the sequence used by Tirrell indicates that this central 'block' region remains a flexible, random coil in solution.[46]

We observed that the domain structure of the Tirrell hydrogel proteins—with a central disordered region flanked by helical regions—resembled a simple version of the domain structure of PopZ, which also contains a central disordered region flanked by helices (Figure 19). Given the understanding that unipolar PopZ assembly in *E. coli* is driven by oligomerization and exclusion from the chromosome-containing nucleoid region, we hypothesized that simple, synthetic proteins resembling Tirrell's triblock proteins might also oligomerize in *E. coli* and be excluded from the nucleoid region.[28] If successful, this would provide a micron-sized assembly that could be used to organize biochemical processes in bacteria such as gene regulation and metabolic pathways. Moreover, we were inspired by the monopolar assemblies of PopZ which enable asymmetric cell division. Past studies have suggested that PopZ's high propensity to self-assemble may direct assemblies to be monopolar versus accumulating at both cell poles (i.e. assembly growth kinetics

exceed assembly nucleation kinetics). If this is a determining factor, we further hypothesize that the Tirrell hydrogel assemblies may also preferentially accumulate at one cell pole.

2.1.2 Synthetic Condensate Designs

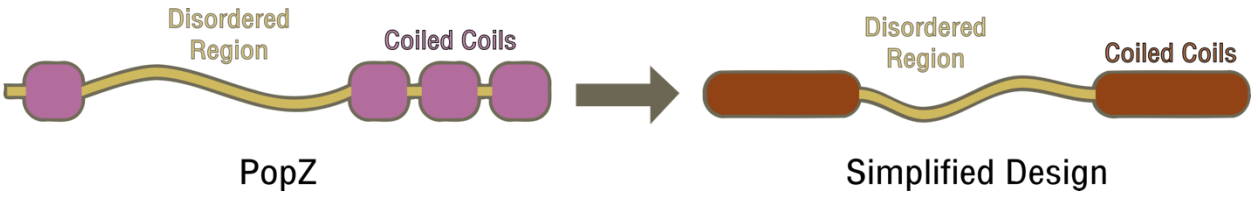

Figure 19: Rationale for synthetic condensate designs. A rough layout of the domain structure of PopZ, with blocks representing helices and lines representing regions of disorder. We simplified the domain structure into a 'triblock,' mimicking the design of the Tirrell group hydrogel proteins, with only two helices and one central region of disorder when planning our constructs.

We modeled our condensate design after the Tirrell group's triblock structure, with mismatched helical bundles separated by a flexible, charged linker (Figure 19). For the central disordered region, we used eight repeats of a linker designed by Waldo et al., GSAGSAAGSGEF, hereafter referred to as the Waldo linker.[51] This linker is flexible and has a charge distribution similar to that of the linker used by the Tirrell group, AGAGAGPEG (Figure 20). However, the Waldo linker was designed to reduce homologous repeats in the DNA coding sequence.[43,51] This is an important feature of the linker: repeating amino acid sequences are a common feature of disordered protein regions, but their presence can make DNA synthesis a challenge.[52] Minimizing nucleotide repeats as much as possible while still using a sequence with repeating amino acids enabled us to successfully synthesize our designs. Of note, while the charge distribution of the

Waldo linker is similar to that of the linker used by the Tirrell group, both of these linkers are far less negatively charged than PopZ's PED linker (Figure 20). The amount and distribution of charge through the amino acid sequence may impact the mechanism of self-assembly, its ability to recruit client proteins, and its material properties..[53,54] Thus, our constructs may have material properties more similar to those of the Tirrell group hydrogels than that of PopZ condensates.

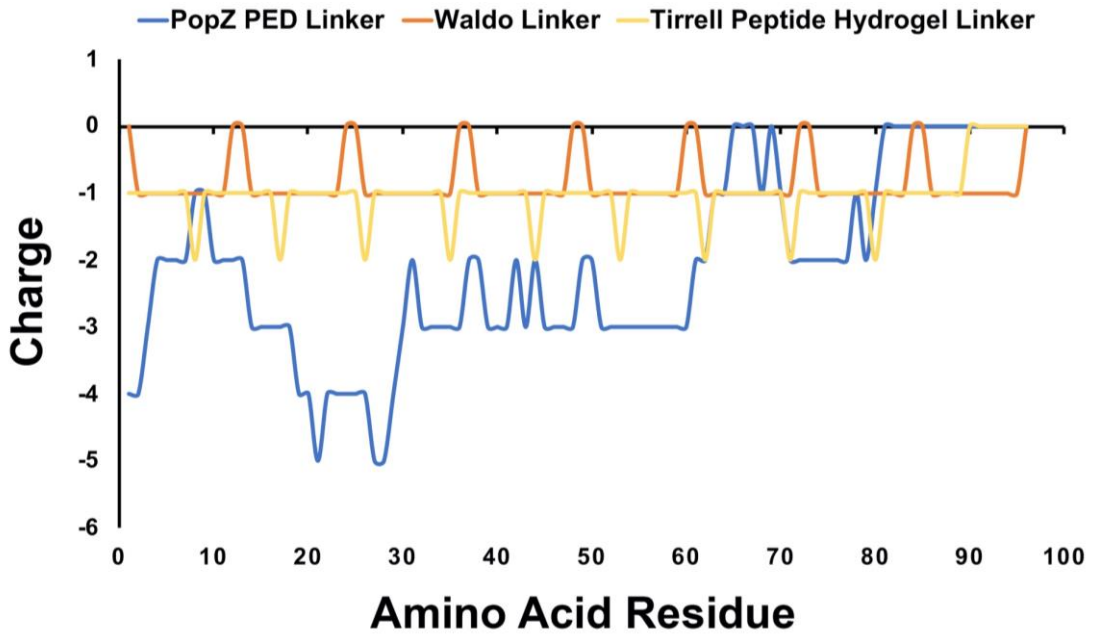

Figure 20: Net charge of disordered linker regions A plot of the net charge across the amino acid sequence of the Waldo Linker, the Tirrell Linker, and the PED disordered central region of PopZ. Using a reference pH of 7.0, positive amino acids (K, R, H) were given a nominal charge of +1, negative amino acids (E, D) were given a nominal charge of -1, and all amino acids were given a charge of 0. The sum of the nominal charges in an 11 amino acid window centered around a single amino acid were used to generate the total charge around that amino acid.

When selecting coiled coils to flank the disordered region of our constructs, we considered the importance of valency in the formation of phase separated structures.[17] The Rosen group demonstrated that increasing the number of binding units between individual proteins in a

condensate increased the concentration of molecules moving into the phase-separated assembly.[17] Thus, we hypothesized that valency of binding would impact the properties of our synthetic condensates, and chose several different coiled coil binding units to test this idea (Figure 21).

We initially selected the same coils used by the Tirrell group in an early triblock protein design.[43] Of note, these binding units are more precisely defined as helical bundle structures rather than traditional coiled coils. Helical bundles are differentiated from coiled coils by their wider hydrophobic face—they often have nonpolar residues at the e and g positions of the heptad, whereas coiled coils have nonpolar residues only at the a and d positions.[49] Due to their narrower hydrophobic face, coiled coils normally assemble in bundles of up to four, while a wider nonpolar face enables helical bundles to assemble in larger four- and five- member groups.[49] The bundles we used, copied from the Tirrell constructs, include a pentameric bundle derived from the cartilage oligomeric matrix protein (COMP)—which we refer to as HB5 (helical bundle 5)—and a tetrameric coiled coil—referred to as HB4 (helical bundle 4)—whose design was inspired by the residues at the a and d heptad positions of the Jun oncogene product.[43,55] Both of these coils feature six heptad repeats, but HB5 oligomerizes into a pentamer in parallel while HB4 oligomerizes into a tetramer in an antiparallel fashion.[43]

To more fully test our hypothesis that valency of binding will impact the properties of our condensates, we also selected two traditional coiled coils that form a homodimer and a homotrimer which we'll refer to as HB2 (helical bundle 2) and HB3 (helical bundle 3). These coils were designed *de novo* by the Woolfson group, they are slightly shorter than the HB4 and HB5 bundles—only four heptad repeats instead of six—and they both assemble in parallel.[56] The relative length of HB2 and HB3 compared to HB4 and HB5 may impact the relative binding stability of the coils—though the K_d of the exact HB4 and HB5 designs has not been

experimentally determined. The Woolfson group previously demonstrated that increasing the number of heptad repeats by just a single heptad resulted in a 600-fold improvement in the K_d of their *de novo* coils.[57]

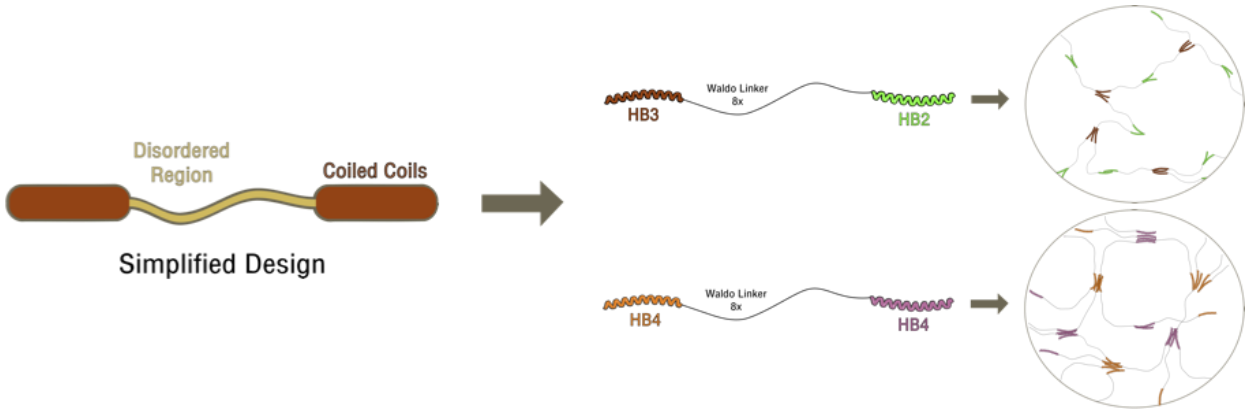

Figure 21: Selection of coiled coils for constructs to test valency of binding. We selected four helical binding units of varying assembly numbers to test the hypothesis that the valency of oligomerization at each end of the protein will impact the material properties of the resulting gel-like condensate. Those constructs with HB4 and HB5 should assemble into denser networks than those containing HB2 and HB3.

2.2 Synthetic Coiled Coil Structures in *E. coli* Assemble at the Cell Poles

To test our hypothesis that synthetic mimics of PopZ will self-assemble at the cell poles in *E. coli*, we expressed both our HB2/HB3 and HB4/HB5 constructs (Figure 21). Consistent with past studies, we observed that PopZ-FP assemblies accumulated robustly at a single cell pole.[27,42] In contrast, the HB2/HB3 and HB4/HB5 constructs formed foci at both poles (Figure 22). Cells expressing the HB2/HB3 condensate displayed monopolar foci in greater numbers than those expressing the HB4/HB5 condensate (Figure 22). Therefore, simple peptide hydrogels provide a mechanism for formation of micron-sized assemblies at the cell poles. However, in contrast to the

PopZ assemblies, we observed that the synthetic peptide hydrogel assemblies readily accumulated at both cell poles.

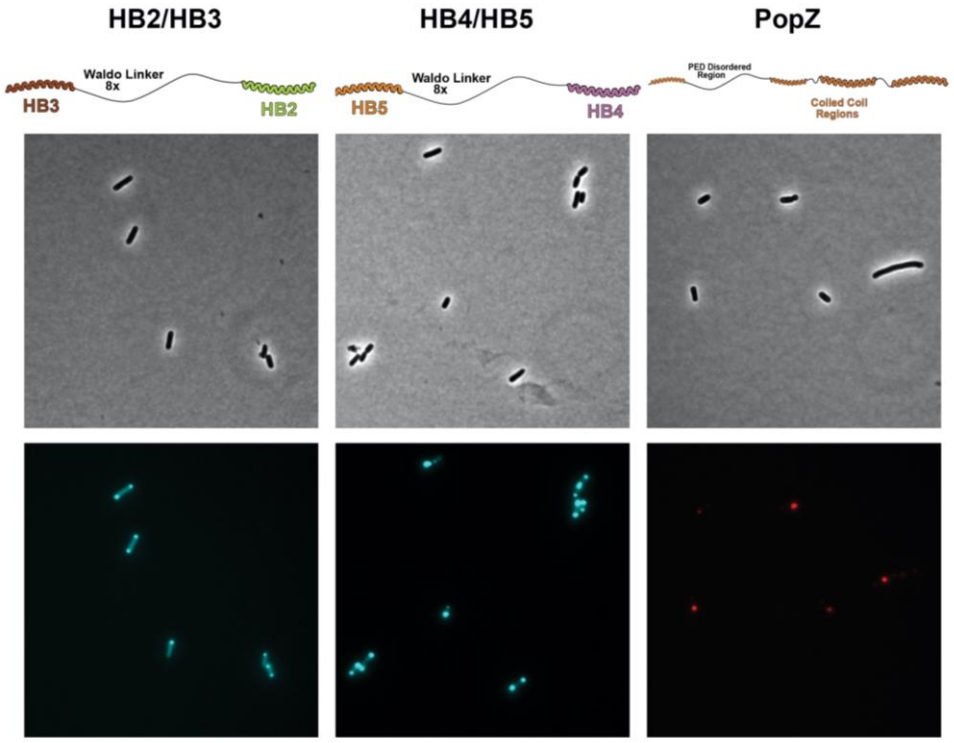

Figure 22: Synthetic coiled coil structures assemble in *E. coli* Both our HB2/HB3 construct and our HB4/HB5 construct assemble into foci at the cell poles in *E. coli*. This localization occurs at both poles of the cell, while PopZ assembles at only a single pole in *E. coli*.

Interestingly, we observed that foci formation was impacted based on the position of the fluorescent protein fusion site. When the fluorescent protein was attached to the N-terminal end of our HB2/HB3 construct next to the HB2 coil, foci formation was inhibited, and the protein was diffuse throughout the cytoplasm (Figure 23A). With the fluorescent protein fused to the C-terminal end next to HB3, however, the construct was able to form foci (Figure 23A). We also created scrambled scaffolds—placing HB4 and HB5 together on one side of the Waldo linker—and observed that positioning the fluorescent protein on the C-terminal end of the construct close

to the helical bundling sequence HB4/HB5 inhibited foci formation (Figure 23B). In contrast, placing the HB4/HB5 helical bundle on the N-terminal end of the construct and separating it from the fluorescent protein with nine repeats of the Waldo linker enabled the scrambled construct to form foci (Figure 23B). These observations support the idea that steric clashes between the fluorescent protein and the helical bundles inhibit assembly of the proteins into foci; however, without creating a construct with CFP and HB3 at the N-terminal end of an HB2/HB3 protein (N-CFP-HB3-Waldo8x-HB2-C), we can't rule out the possibility that protein misfolding of HB2 prevented oligomerization in our N-terminal CFP-HB2-Waldo-HB3 construct. Additionally, we need to perform a Western Blot to confirm similar protein expression levels between constructs. Because of these observations, though, we attached fluorescent proteins to the C-terminal end of our constructs next to the higher bundling coiled coil in all our designs.

Another interesting observation is that the scrambled construct with an N-terminal HB4/HB5 bundle forms assemblies at the mid-cell as well as at both of the cell poles (Figure 23B, bottom panel).These assemblies may localize to the mid-cell through interactions with the FtsZ septal ring complex, which localizes to the same mid cell position in *E. coli* as these mid-cell foci formed by our synthetic construct.[58,59] It appears that the FtsZ ring assembles and matures into a septal ring complex, with requisite colozalization of the binding partners necessary for division, because we observe invagination of the membrane at the division plane. This invagination is a sign that the mature septal ring complex has assembled, but that its contraction leading to full septation has not yet begun.[58] We think that our synthetic construct localizes to and interferes with the contraction of the septal ring complex because we observe elongated cells with many points of constriction when this construct is expressed (Figure 24). This interference is unique to the

construct with HB4 and HB5 placed side-by-side on the N-terminal end of the peptide and does not occur when HB4 and HB5 are separated from one another by repeats of the Waldo linker.

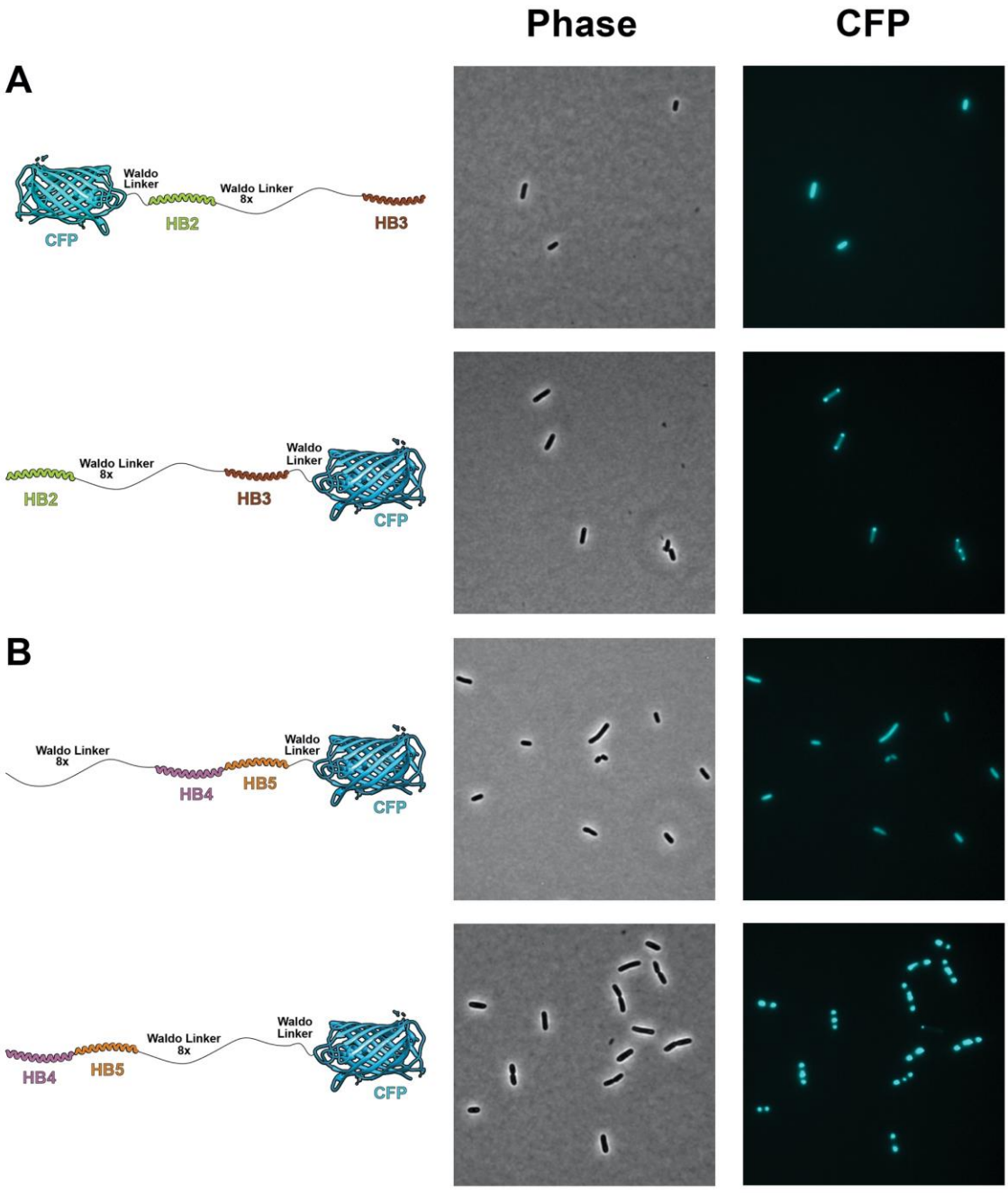

Figure 23: Steric clashes prevent assembly of coiled coil constructs in *E. coli* (A) Positioning CPF at the N-terminal end of our HB2/HB3 construct, close to the HB2 bundle, prevented foci formation. When CFP was placed at the C-

terminus next to the HB3 bundle, the constructs were able to assemble into foci. (B) When HB4 and HB5 were placed close together at the C-terminal end of the construct next to CFP, the construct failed to assemble into foci. When these bundles were placed at the N-terminal end of the construct separated from CFP by nine copies of the Waldo linker, foci formation occurred.

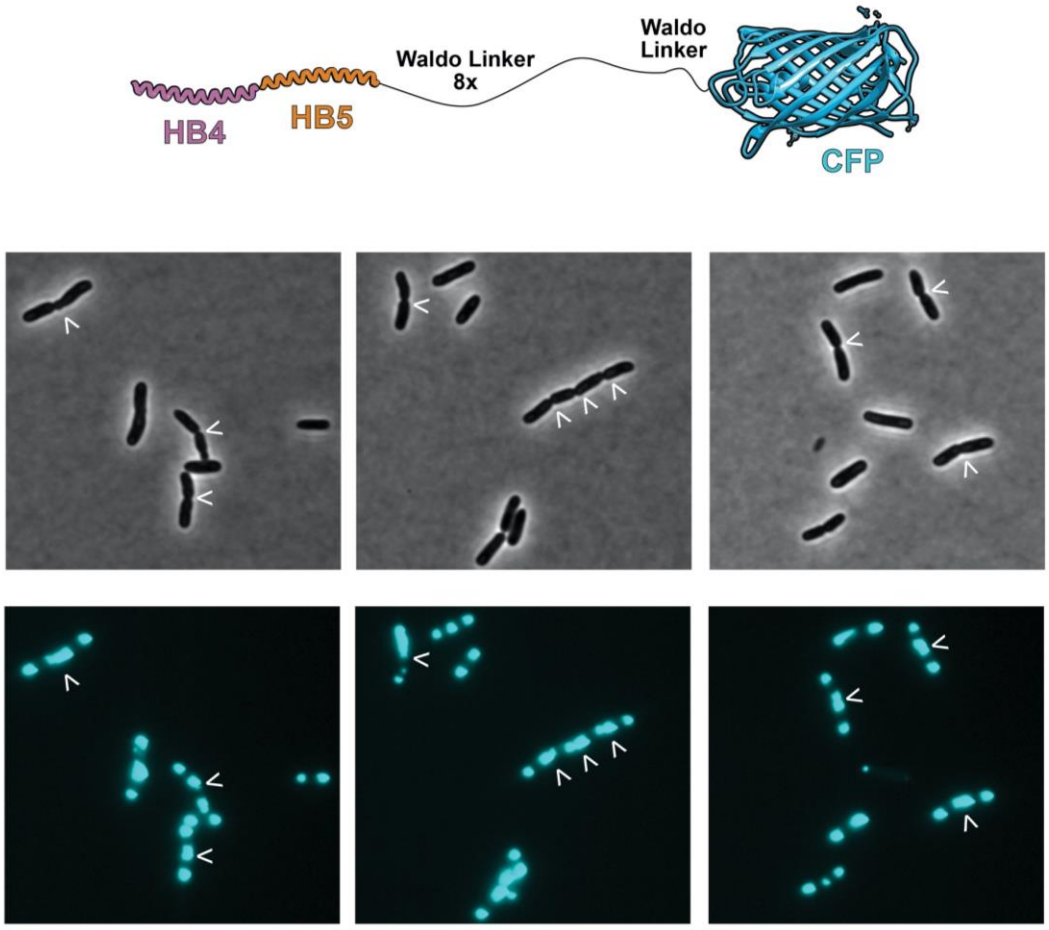

Figure 24: A synthetic coiled coil construct binds the midcell in *E. coli* A scrambled coiled coil construct (top) was expressed in *E. coli* for two hours before imaging. White arrows indicate points of invagination without complete septation and the corresponding synthetic construct assemblies at these positions.

In order to further explore the reasons our constructs formed foci at both poles—instead of at just one pole like PopZ—we considered other mechanisms that may drive PopZ to assemble at one cell pole (Figure 25). Past studies have shown that PopZ in both *C. crescentus* and *E. coli*

excludes ribosomes from the microdomain it forms at the cell poles.[21,59,60] Therefore, we hypothesized that PopZ's monopolar accumulation may be the result of competition between ribosomes and PopZ to occupy the two nucleoid occluded regions of the cell. To test this idea, we hypothesized that the size of the linker between the helical bundles would adjust the peptide hydrogel's pore size to either permit or exclude ribosomes. Thus, we decreased the size of the linker to test if linker length impacts bipolar versus monopolar accumulation of the peptide hydrogel constructs. We hypothesized that if ribosomes were excluded from both the nucleoid region and the synthetic condensate, that the ribosomes would occupy one cell pole and our synthetic condensate the other. We observed that reducing the linker size led to a slight increase in the number of cells exhibiting monopolar formation of synthetic assemblies, but this effect was more pronounced for the HB2/HB3 construct, which already displayed greater monopolarity. Reduction in pore size by half increased monopolar formation of the HB2/HB3 construct from 64.7% to 74.3% of observed cells and increased monopolar formation of the HB4/HB5 construct from 27.3% to 27.9% of observed cells (Figure 25).

Alternatively, we considered the possibility that expression level dictates the transition from unipolar to bipolar assembly of our peptide hydrogel constructs. We hypothesized that our synthetic condensates might assemble in a unipolar fashion at low concentration levels and transition to bipolar assembly at high expression levels. However, we observed the assembly of the HB2/HB3 construct every thirty minutes for the first two hours following induction and found bipolar assembly even after only thirty minutes of expression (Figure 26). This suggests that monopolar vs. bipolar localization of our peptide hydrogel constructs is due to the construction and intrinsic properties of the peptide rather than expression level. In comparison, PopZ polar localization is also independent of expression level, though it instead maintains unipolar

localization even when overespressed.[21] To confirm expression level independence of our synthetic assemblies, future studies should include Western blots of expression over time.

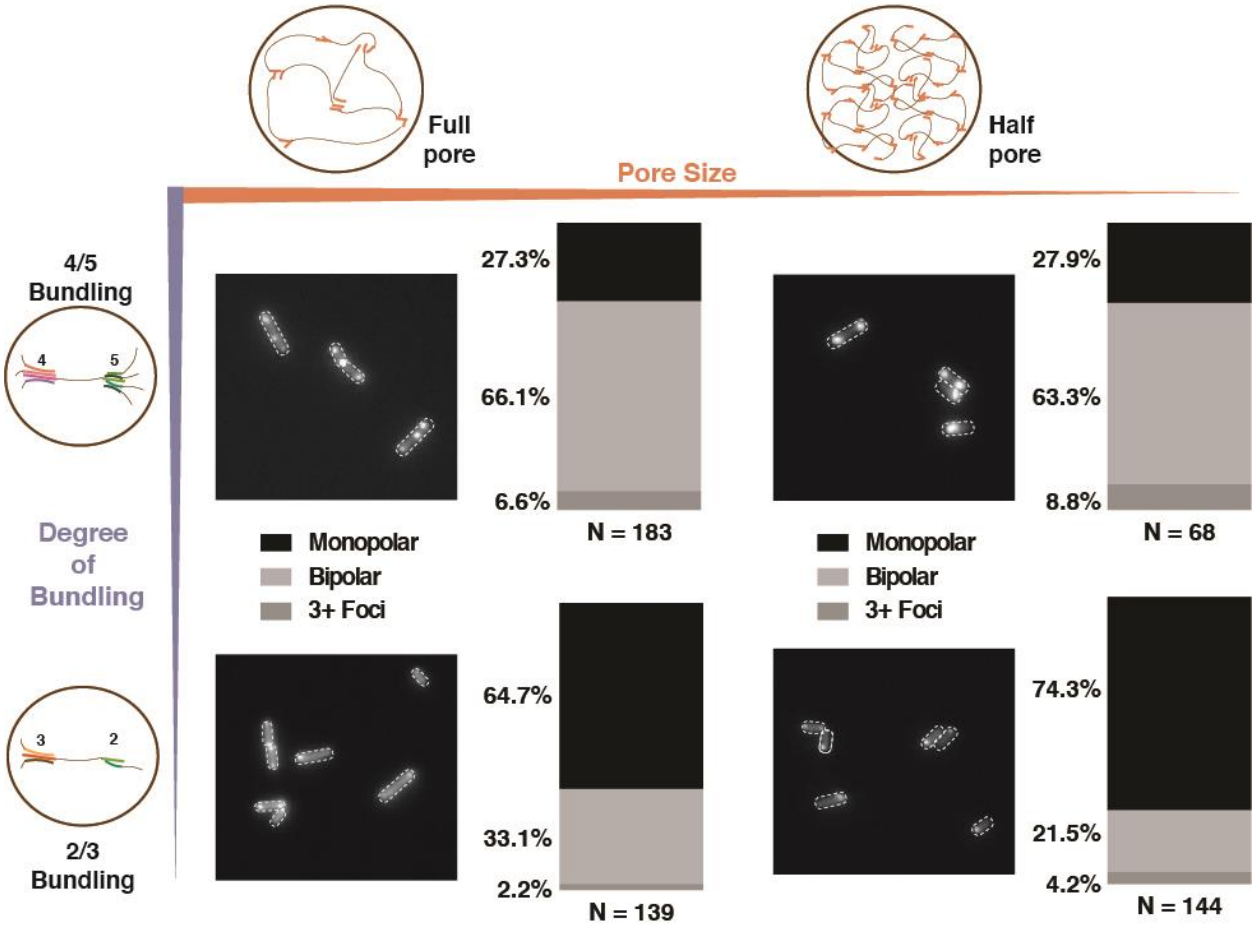

Figure 25: Reducing bundling and pore size increases monopolarity of synthetic constructs The synthetic construct with the lowest bundling number and smallest pore size most closely resembled the unipolar localization of PopZ.

Our peptide-hydrogel assemblies partially mimicked PopZ in that they did localize to the cell pole, but they did not achieve the complete unipolar localization observed when PopZ is expressed in *E. coli*.[27,42] These results support our hypothesis that oligomerization by gel-like

proteins results in localization to the cell poles in *E. coli*; however, they point to additional factors responsible for unipolar localization of PopZ that are missing from our synthetic constructs.

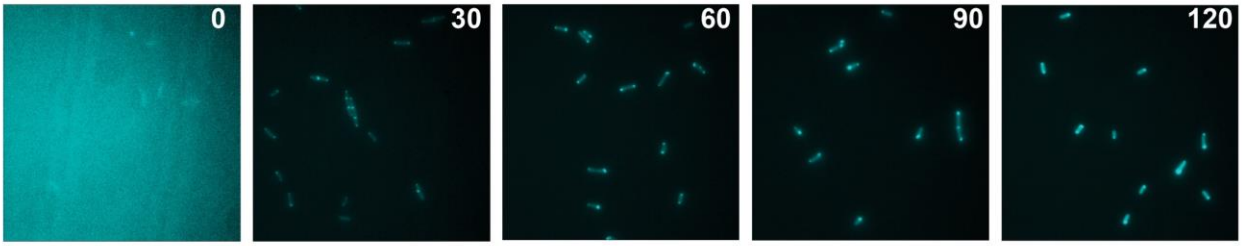

Figure 26: Low expression levels don't produce unipolar synthetic construct assemblies After induction of the HB2/HB3 synthetic coiled coil construct, cells were imaged every thirty minutes (time of image in white). Cells displayed bipolar foci formation after just 30 minutes of induction, indicating that high concentration is not responsible for bipolar assembly.

In our studies of the peptide hydrogel design, we considered the impact of helical bundle valency and linker length upon the accumulation of the protein at one or two cell poles. Our studies indicated that helical bundle valency has a stronger effect upon the percent monopolar (64.7% versus 27.3%) than linker length (64.7% vs 74.3%). These differences may also be influenced by total protein levels; therefore, future western blot analysis will be needed to compare protein levels to consider their influence upon the degree of cells that exhibit monopolar localization. As well, to test the ribosome-PopZ competition hypothesis additional experiments will be needed to visualize assembly and position of ribosomes relative to PopZ in *E. coli*. It also possible that the charge of the central disordered region, which is less negatively charged than the PopZ PED linker, could be changed to improve the monopolarity of synthetic assemblies. The presence of sufficient negatively charged amino acids in the disordered PED region is critical for PopZ to function normally, so future studies could investigate the effect of various charge concentrations on condensate polarity.[44]

2.3 Synthetic Coiled Coil Structures in *E. coli* Localize to the Cell Poles via Nucleoid Occlusion

We designed our synthetic constructs to localize to the pole via nucleoid occlusion, the mechanism by which PopZ achieves its polar localization.[21,35] For PopZ, nucleoid occlusion occurs because small PopZ assemblies throughout the cell are able to oligomerize together and form large assemblies in polar regions where the nucleoid is not present.[21,61] As our synthetic condensates oligomerize, we hypothesized they would preferentially assemble at the cell poles through nucleoid occlusion.

To test if this is the mechanism at work in the polar localization of our synthetic condensates, we followed the example of Laloux et al., treating *E. coli* cells expressing our constructs with cephalexin and staining them with DAPI to visualize the position of DNA-containing nucleoid regions relative to our synthetic assemblies.[21] Treatment of *E. coli* cells with cephalexin prevents cell division, but not replication of the chromosome, creating elongated cells containing many nucleoid regions. As expected, we observed assembly of both our HB2/HB3 and our HB4/HB5 constructs in many nucleoid-free regions throughout the elongated cell (Figure 27). These results support the hypothesis that nucleoid occlusion is involved in dictating the localization of our coiled coil assemblies. However, further proteomics studies could be performed to determine if the condensates also interact with any native *E. coli* polar landmarks.

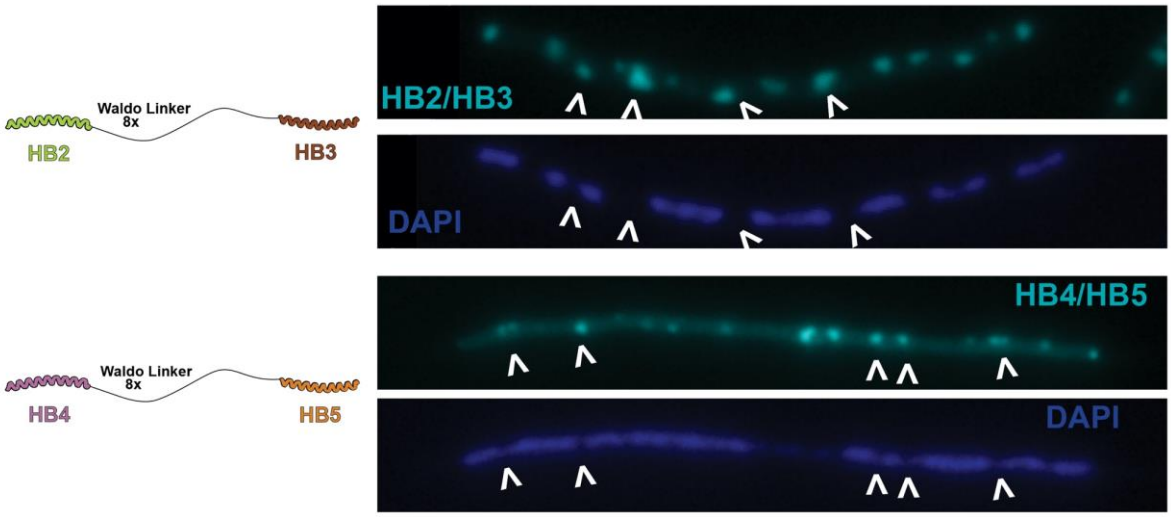

Figure 27: Nucleoid occlusion of synthetic coiled coil constructs *E. coli* cells were treated with cephalexin before induction of HB2/HB3-CFP (top) or HB4/HB5-CFP (bottom). Arrows indicate synthetic construct assembly in DNA-free areas and corresponding gaps between the dark blue nucleoid regions.

2.4 Synthetic Coiled Coil Structures in *E. coli* Recruit and Exclude Client Proteins

Having developed constructs that approximate PopZ's unipolar localization and mechanism of targeting the pole, we next sought to develop a modular approach to recruit client proteins to the synthetic condensates. This will provide evidence that our constructs have the potential to be functional, and have not simply misfolded into aggregated inclusion bodies which are insoluble and largely exclude folded proteins.[28,44,62] To first establish that proteins can enter the synthetic assemblies and show that recruitment of clients is possible, we co-expressed the synthetic condensates with GFP. If GFP was unable to penetrate the synthetic assemblies, we hypothesized, it would be challenging to target client proteins to the domain. However, GFP

diffused freely through the body of the cell and was able to penetrate our synthetic assemblies, so we moved ahead to add recruitment features to our designs (Figure 28).

In order to target client proteins to the synthetic condensate, we selected the *de novo* designed E3/K3 set of coiled coils.[63] This set forms a tight heterodimer with 1:1 stoichiometry at nanomolar affinity, and purification experiments with each coil expressed in *E. coli* lysates indicated that the pair associates only with each other and does not bind native cellular proteins.[63] Because of the small size of the coils—21 amino acids—vs the other longer binding proteins like the SYNZIP family—42 amino acids—we also anticipated minimal steric interruption of condensate properties by these coils.[63,64] Steric interruptions were especially concerning given our previous observations of construct assembly interruptions by fluorescent protein placement (Figure 23).

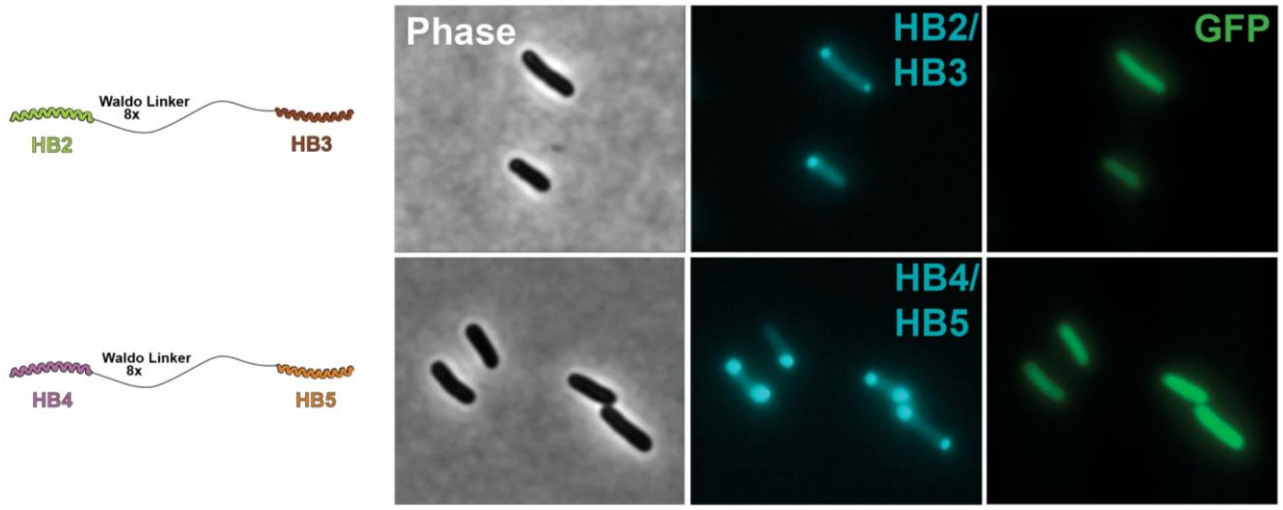

Figure 28: Synthetic coiled coil constructs admit cytoplasmic proteins. Synthetic constructs were expressed simultaneously with GFP for 2hr before imaging. Both the HB2/HB3 and HB4/HB5 constructs admitted GFP.

To create synthetic constructs capable of recruiting clients, we inserted two copies of the E3 coil into the central disordered region of the HB4/HB5 construct (Figure 29). E3 was selected

for insertion into the condensate protein because it does not form homodimers, whereas K3 coils homodimerize at concentrations above 11 mM.[63] At this concentration, homodimerization is unlikely to impact assembly of our constructs, but we chose to attach the K3 coil to our recruited client protein initially to minimize any potential homodimerization. To visualize client recruitment, we selected the Venus fluorescent protein as a client and attached the K3 coiled coil to it via a single copy of the Waldo linker (Figure 29).

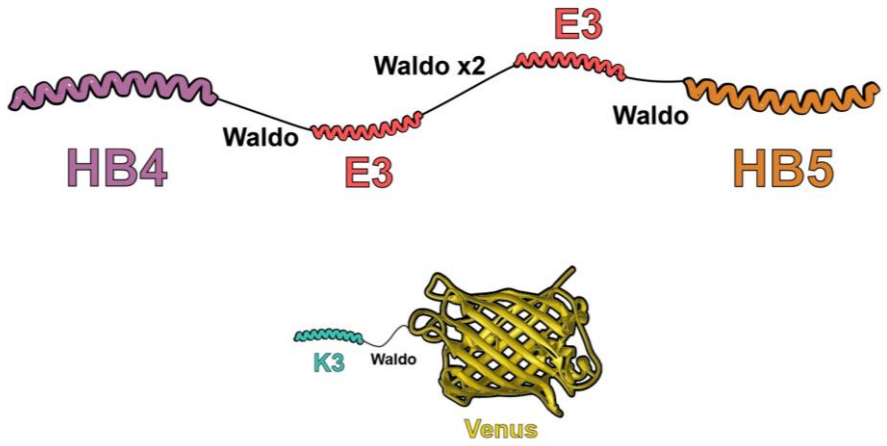

Figure 29: Design of recruitment synthetic coiled coil and client proteins In order to recruit a fluorescent protein client to our synthetic scaffold assemblies, we added two copies of the E3 coiled coil into the central, disordered waldo linker. These coils were able to recruit the fluorescent client, Venus, which had E3's binding partner attached N-terminally via one copy of the waldo linker.

We then tested the ability of the recruitment construct to bind and concentrate the tagged client protein by co-expressing the recruitment coiled coil construct and the client (Figure 30A). The recruitment construct still formed polar foci, despite addition of the E3 recruitment coils into the central disordered region, and the mVenus client protein was concentrated into the polar regions of these cells (Figure 30A). This concentration did not appear to be the result of possible

K3 dimerization, because we observed diffuse K3 throughout the 74 cells observed when it was expressed alone (Figure 30A). Average fluorescence intensity profiles along the longitudinal axis of the observed cells showed K3-Venus clustered in the recruitment construct foci in co-expression cells and diffuse through the cytoplasm when alone (Figure 30B). This indicates that our synthetic construct can successfully recruit and concentrate a client protein within the cytoplasm.

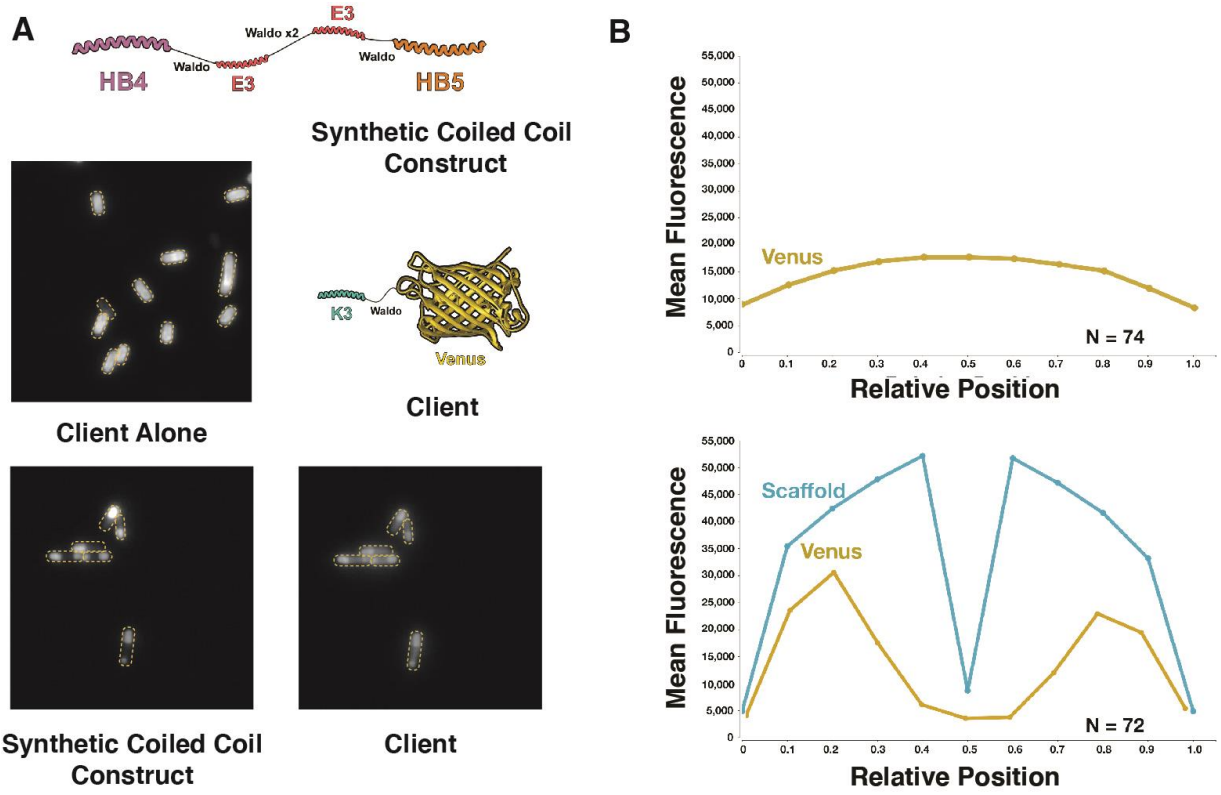

Figure 30: A synthetic coiled coil construct is able to recruit a fluorescent client (A) The K3-tagged Venus client protein was expressed for two hours either alone or co-expressed together with a coiled coil construct containing the E3 recruitment coil (K3's binding partner). When expressed alone, the Venus client protein is diffuse through the cytoplasm. Expression together with the coiled coil recruitment construct results in concentration of the Venus client in the coiled coil construct foci. (B) Fluorescence intensity profiles normalized to cell length show the average distribution across the cell body of the Venus client protein alone, or the client protein co-expressed with the CFP tagged synthetic scaffold construct.

Another important feature of biomolecular condensates is the ability to selectively exclude proteins, which often occurs through electrostatic charges in the condensate and on the excluded proteins.[18] The addition of the E3 coiled coil to our recruitment condensate increased the negative charge of the condensate—E3 has six additional glutamic acid residues—and concentrated this charge into two small regions in the disordered linker (Figure 31A, B). Conversely, addition of the K3 residue would create regions of concentrated positive charge in the linker, as K3 has six lysine residues at the same coil positions as the glutamic acid residues in E3 (Figure 31A, B).[63] To determine if our scaffold would exclude proteins selectively, we swapped the E3 coiled coils for K3 coiled coils, and co-expressed the K3 condensate with the K3 tagged Venus client. When both condensate and client contained positively charged coils, the synthetic condensate excluded the client from the polar region of the cell (Figure 31C).

These experiments establish the ability of our synthetic condensates to perform a client recruitment function similar to that of PopZ. A protein of neutral charge, as well as one specifically targeted to the condensate, is able to enter the polar condensate domain freely, while a protein of incompatible charge can be purposefully excluded from the condensate. This points toward the ability to selectively control the domain within our synthetic assemblies.

With this evidence that our constructs are capable of recruiting and excluding a fluorescent client, further work should be done to quantify this recruitment and exclusion. This could be done by calculating a percentage of the client protein present in the coiled coil construct versus that in the cytoplasm. Such calculations in conjunction with a titration examining the ratio of scaffold to client would enable us to determine the optimal expression levels for recruitment using our initial designs. In addition, variations on the design of the recruitment constructs that might improve its recruitment capabilities could be tested and quantified. We haven't yet tested the effect of pore

size or number of recruitment coils on the ability of the construct to recruit clients; however, these factors might have an impact on client residence time in the assembly—in the case of a smaller, more constricting pore size—or on client:scaffold stoichiometry in the case of varying numbers of recruitment coils in the synthetic assembly.

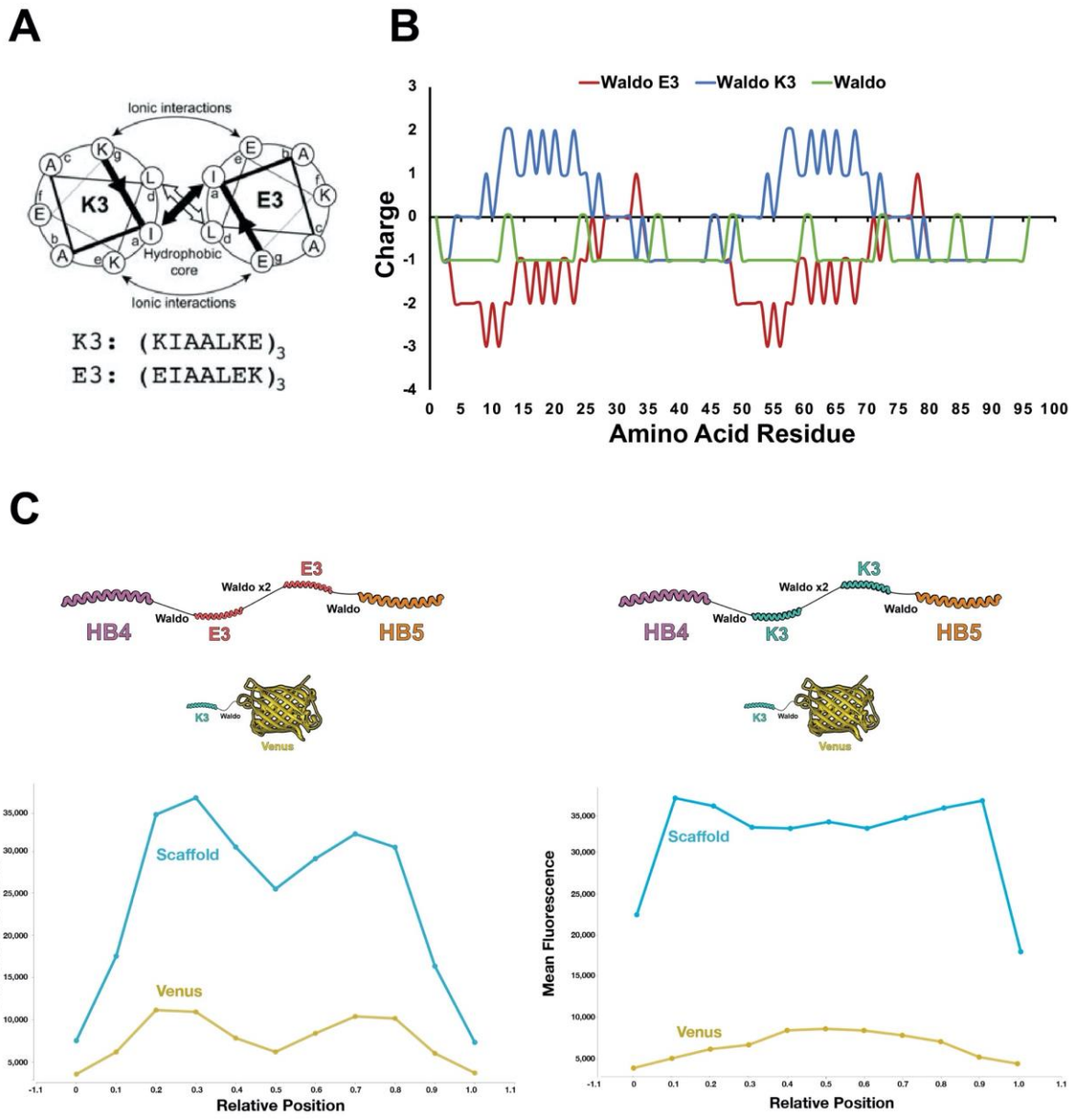

Figure 31: Synthetic coiled coil constructs can use electrostatics to exclude a fluorescent client A helical wheel representation of the E3/K3 coiled-coil. Reprinted by permission from John Wiley and Sons, Charles, M., Perez et al.

(2001). Proceedings of the National Academy of Sciences, 98(17), 9871–9876. (B) Net charge distribution of the various disordered regions placed between oligomerizing helical bundles in this work. Waldo Linker: $(GSAGSAAGSGEF)_{8,}$ Length = 96 amino acid residues; Waldo E3: Waldo-E3-$(Waldo)_2$-E3-Waldo, Length = 90 amino acid residues; Waldo K3: Waldo-K3-$(Waldo)_2$-K3-Waldo, Length = 90 amino acid residues. Using a reference pH of 7.0, positive amino acids (K, R, H) were given a nominal charge of +1, negative amino acids (E, D) were given a nominal charge of -1, and all amino acids were given a charge of 0. The sum of the nominal charges in an 11 amino acid window centered around a single amino acid were used to generate the total charge around that amino acid. (C) Fluorescence intensity profiles normalized to cell length show the average distribution across the cell body of CFP tagged synthetic scaffold constructs and the venus client protein. (Left) Fluorescence intensity profile of the E3 synthetic construct with a negatively charged linker expressed with positively charged K3 tagged Venus. (Right) Fluorescence intensity profile of the K3 synthetic construct with a positively charged linker expressed with positively charged K3 tagged Venus.

2.5 Possible Multi-Phase Structures formed between PopZ and Synthetic Coiled Coil Constructs

With the goal of creating synthetic structures that act as physical landmarks for asymmetric cell division in *E. coli*, we sought to determine if our coiled coil constructs would act as a second polar landmark alongside PopZ. We coexpressed PopZ with both the HB2/HB3 and HB4/HB5 constructs, hypothesizing that the synthetic construct would assemble at one cell pole and the PopZ condensate at the other. Instead, we observed assembly of the PopZ condensate and our synthetic constructs occurring largely at the same cell pole (Figure 32). It appeared that our synthetic construct did form separate assemblies, in that we observed two small foci forming side-by-side at the one pole when PopZ was expressed with each of the synthetic constructs (Figure 32). This occurred in ~25% of the cells counted when PopZ was expressed with the HB2/HB3 construct,

and in ~11% of cells counted with coexpression of the HB4/HB5 synthetic construct with PopZ (Figure 32). This supports the idea that our constructs phase separate from the PopZ condensate, because they were excluded from the PopZ condensate despite cytoplasmic proteins having previously been shown to diffuse through it.[44] In addition, we frequently observed the synthetic assemblies surrounding a smaller PopZ condensate; however, it is impossible to tell if this is separate from side-by-side formation of the two condensates without three-dimensional information. More detailed, three-dimensional information might also reveal the presence of PopZ condensates on the opposite side of synthetic condensates in the groups of cells appearing to express only the synthetic condensate (Figure 32). However, given that this degree of phase separation is at or near the limits of standard fluorescence microscopy resolution, future superresolution microscopy will be needed to characterize the co-assembly of these scaffolds. In particular, future studies should examine the effect of expression order on condensate assembly, as well as looking at assembly of both condensates in real time.

Although our goal was to create a synthetic condensate that would localize to the opposite pole of PopZ in *E. coli*, our creation of structures that are phase-separated from PopZ still represent progress towards that goal. While we may not be able to leverage the two condensates to promote asymmetric cell division, they may offer the potential to partition biochemical processes into distinct three-dimensional zones. This could be used, for example, to insulate metabolic pathways that may exhibit shared intermediates or branched pathways. This could also influence phosphorylation cascades by segregating kinase substrates within distinct condensates. Future efforts will be needed to demonstrate partitioning of clients and leverage the ability to segregate proteins.

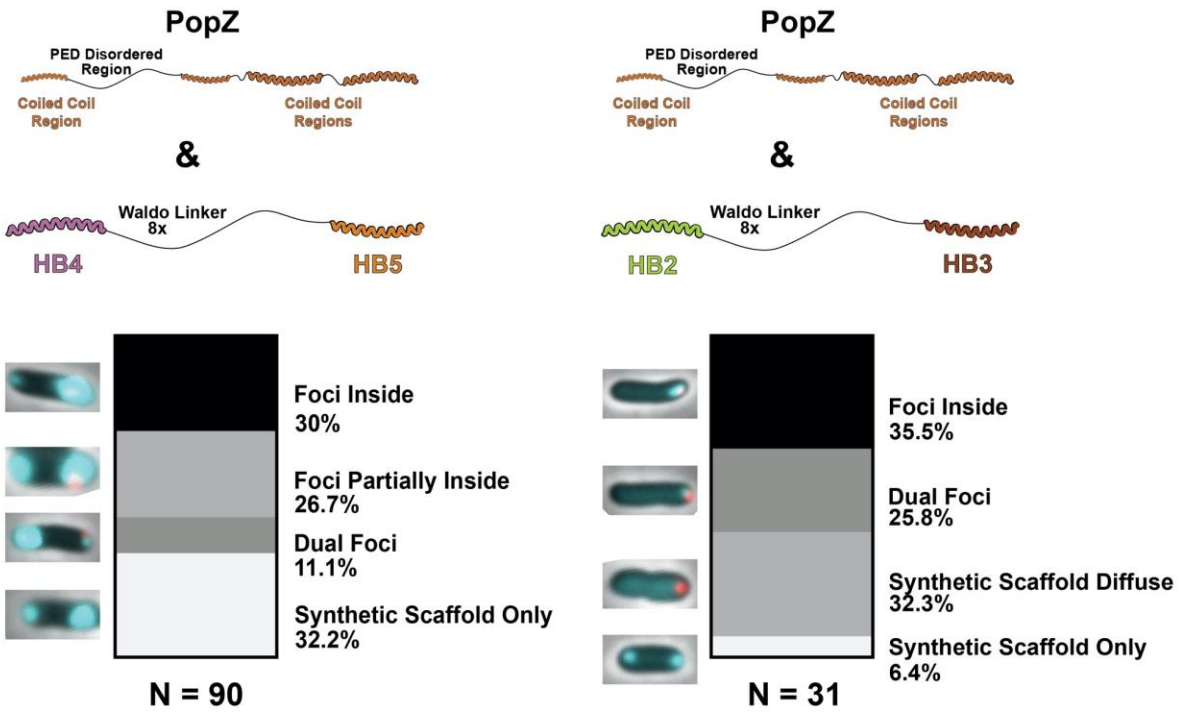

Figure 32: Synthetic coiled coil constructs form separate assemblies when co-expressed with PopZ PopZ and synthetic coiled coil constructs were expressed for two hours prior to imaging. They two condensates formed foci beside and within one another, as well as occasionally inhibiting each other's assembly.

2.6 Conclusions and Future Directions

In these experiments, we demonstrated that peptide hydrogel constructs could form biomolecular condensates in bacteria. While it remains unclear if the synthetic biomolecular condensates exhibit liquid-like behavior or solid-like assemblies, we were able to design a construct that assembled in a largely monopolar fashion in *E. coli,* and we were able to selectively control the client proteins admitted to the synthetic construct assembly. Our designs even displayed evidence of phase separation from PopZ when co-expressed, a positive step towards creating a separate, pole-localized biomolecular condensate that could operate orthogonally and potentially

in conjunction with PopZ to regulate biochemical pathways. Thus, we have engineered a synthetic 3-dimensional zone in bacterial cells that could be used to organize and coordinate biochemical pathways.

However, these results point towards mechanistic questions about how PopZ is able to assemble at a single pole in *E. coli* that remain unanswered. Because our synthetic constructs fell short of the near perfect unipolar assembly that PopZ displays in *E. coli*, it is clear that more is at work in this localization pattern than just exclusion of the condensate from the nucleoid region. Given the importance of the charged, disordered PED region to PopZ functionality, it is possible that testing different charges and patterns of charge distribution within the disordered region would result in synthetic condensates with a more monopolar localization.[44] When we introduced the E3 and K3 coils into the disordered region of our condensates for recruitment, we dramatically altered both the charge and the degree of structure of the disordered linker; however, we only tested this charged region with the HB4/HB5 coiled coils. In future work, then, it is imperative to test this charged region with the HB2/HB3 pair to hopefully marry the greater monopolarity displayed by condensates with those coils together with recruitment functions. It is possible that the introduction of more charged residues into the HB2/HB3 linker would increase monopolarity of the already-close HB2/HB3 construct with a small pore to maximize the degree of monopolarity

Much also remains unclear about the exact mechanistic details of our own synthetic assemblies. By examining our 'scrambled' scaffolds—with HB5 and HB4 next to each other instead of separated by the linker—we began to test the role of different layouts in the assembly of synthetic condensates. Given the larger proportion of mid-cell condensate assembly in these scrambled constructs, it appears that the orientation of parts in condensate proteins is important. Only with examination of each scaffold part individually—as well as of smaller, two-part

constructs—will the real role of each part and the optimal layout of parts next to one another become clear, however.

Future work must also define the material properties of our synthetic constructs, which we designed in hopes that they would form biomolecular condensates. Our observations of the permeability of our constructs and their ability to recruit and exclude client proteins support the idea that our constructs behave as condensates. To truly feel confident in this assignment, however, it will be necessary to examine the diffusive properties of our constructs. Structures classified as biomolecular condensates display a spectrum of fluid-like properties, from those that behave as liquids to those with more gel-like diffusive properties. These properties are commonly assessed via fluorescence recovery after photobleaching (FRAP) of purified bacterial proteins *in vitro* or by fluorescence loss in photobleaching (FLIP) of bacterial proteins *in vivo*.[29,30,44,65] Ideally, properties of our synthetic condensates will be assessed via both methods, both to confidently assign our constructs to the group of biomolecular condensates and to understand how changes in condensate branching and linker charge impact the material properties of our synthetic condensates.

With a clear understanding of the mechanistic details of both our synthetic condensates and PopZ, we hope that our synthetic condensates will prove a useful tool in the biotechnology box. If we can succeed in developing a synthetic condensate into a second polar landmark in *E. coli*, we could build off of the work of Mushnikov et al in which PopZ was used to generate asymmetric cell division in *E. coli* by setting up a c-di-GMP gradient.[39] With a second polar landmark, creation of two, ideally switchable, cytoplasmic gradients would enable more diverse daughter cell progeny.

Our synthetic condensates could also be used as platforms for engineering the morphology of *E. coli* to improve bioproduction. Work has been done to increase the size of *E. coli* cells to

improve production quantity and make separation of biomass from product more efficient, but many cell wall and division genes haven't yet been modified in this pursuit.[66] Furthermore, in bacterial developmental biology it has been hypothesized that cell morphology is dictated by localization of cell wall synthesis.[67] However, we currently lack strategies to directly test this hypothesis. As a proof of principle, by recruiting both periplasmic and inner membrane peptidoglycan enzymes to our synthetic condensates, we could increase cell wall construction activity at the cell poles relative to the cell body and create dumbbell shaped *E. coli* cells (Figure 33). These distended cells could be filtered from the from cytoplasmic products using a larger filter size, making easier biotechnology applications requiring isolation of cytoplasmic products, as well as providing insights about the individual functions of peptidoglycan enzymes—many of which are challenging to dissect due to overlapping functions between enzymes.[68]

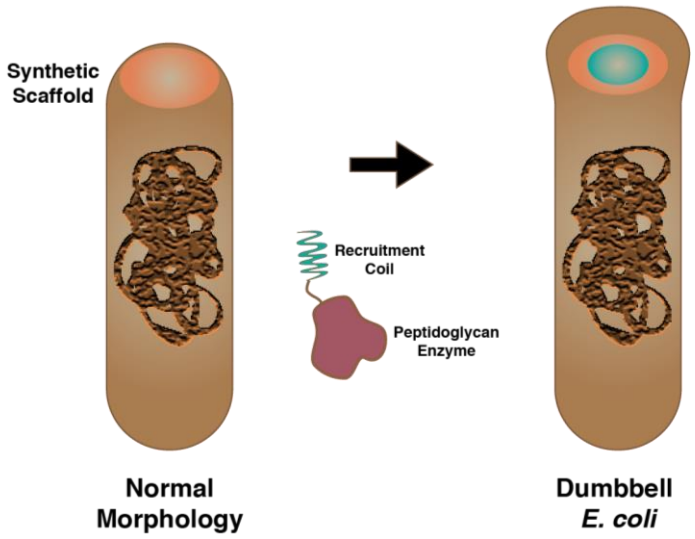

Figure 33: Using synthetic coiled coil constructs to engineer *E. coli* morphology With our synthetic constructs localized to a single pole, we would recruit peptidoglycan enzymes to the synthetic assembly in order to change the morphology of the pole.

Synthetic biomolecular condensates have the capability to function by sequestering key enzymes. We propose that biomolecular condensates could be used to "sequester and release" transcription factors that modulate cell shape. Overexpression of the BolA transcription factor results in cells that are round and lack flagella.[69] Therefore, we propose that recruiting BolA to a synthetic condensate, would inhibit its function and might be able to restore rod-shaped morphology and motility to daughter cells.[69] Expression of the mVenus-K3 fusion as a competitor client might provide a simple mechanism to release the BolA-K3 client from the synthetic scaffold. This would provide a switchable "sequester and release" approach that could also be useful in biotechnology applications.

Through designing synthetic condensates in bacteria, we will continue to learn about the mechanisms by which native condensates assemble and perform roles critical to bacterial life cycle and morphology. With this knowledge, we can peek back in time to the primitive organisms that came before modern bacteria and look to ahead by creating the bacteria of our biotechnological future.

2.7 Experimental Methods

Bacterial Strains

All experiments were performed using DH5- α (Invitrogen) for transformation and storage after plasmid cloning and BL21 (Promega) for expression and imaging.

Plasmid Construction

Restriction enzymes were purchased from Thermo Scientific or Invitrogen. PCR reactions were performed in 50 μL reaction mixtures containing 3% (v/v) DMSO, 1.3 M betaine, 0.3 μM each primer, and 0.2 mM each dNTP, and 1U Phusion High-Fidelity DNA Polymerase (Thermo Scientific). Gibson assembly reactions were performed in 20 μL with 100 ng backbone and a 1:5 backbone:insert ratio, with 0.08 U T5 Exonuclease (New England Biolabs), 1 U Phusion High-Fidelity DNA Polymerase (Thermo Scientific), and 80 U Taq DNA Ligase (New England Biolabs).[70] An annealing temperature of 55 °C for cloning reactions. Plasmids and primers were designed using the j5 Device Editor software.[71] Oligonucleotides and Gene Blocks were synthesized by IDT (Coralville, IA) and DNA sequencing reactions were performed by either the University of Pittsburgh Genomics Research Core or Genewiz (South Plainfield, NJ). DNA oligos, Gene Blocks, and plasmids used in this study are listed in Tables 2-4.

Growth Conditions and Inducer Concentrations

E. coli strains used for microscopy experiments were inoculated from a freezer stock and grown overnight at 37 °C in LB medium. The next morning, strains were diluted 1:100 in fresh LB broth containing appropriate antibiotic. After reaching OD_{600} between 0.5-0.6, protein expression was induced by adding 2 mM Isopropyl β-D-1-thiogalactopyranoside (IPTG) or 10 mM arabinose as appropriate. Cells were induced for 2 hr before immobilization on a 1.5% Ultrapure Agarose (Invitrogen) pad made with LB medium on a microscope slide (VWR).

DAPI Staining and Cephalexin Filamentation

E. coli strains used in nucleoid visualization microscopy experiments were inoculated from a freezer stock and grown overnight at 37 °C in LB medium. The next morning, strains were diluted 1:100 in fresh LB broth containing appropriate antibiotic. After reaching OD_{600} of ~0.3, protein expression was induced by adding 2 mM Isopropyl β-D-1-thiogalactopyranoside (IPTG). For cell filamentation experiments, 20 μg/mL cephalexin was also added with the inducer. Cells were incubated for 1.5 hr and then washed two times in 1x PBS to remove IPTG and cephalexin. Next, cells were fixed in a solution of 2.5% formaldehyde in 30uM 1xPBS for 30 minutes. Finally, cells were stained with 200µl of a 20 mg/mL DAPI stock in 1x PBS, followed by another wash in 1xPBS to remove the stain. Cells were immobilized on a 1.5% Ultrapure Agarose pad made with LB medium on a microscope slide (VWR) for microscopy.

Phase Contrast and Epifluorescence Microscopy

Cells were imaged after being immobilized on a 1.5% LB pad. Phase microscopy was performed by using a Nikon Eclipse Ti-E inverted microscope equipped with an Andor Ixon Ultra DU897 EMCCD camera and a Nikon CFI Plan-Apochromat 100X/1.45 Oil objective. The excitation source was a Lumencor SpectraX light engine. Chroma filter cube CFP/YFP/MCHRY MTD TI was used to image ECFP, Venus, and mCherry. Chroma filter cube DAPI/GFP/TRITC/CY5 was used to image EGFP. Images were collected and processed with Nikon NIS-Elements AR software and ImageJ software.[72]

Fluorescence Intensity Profile Analysis

Strains were imaged using the above methods. The average fluorescence intensity profile using normalized cell length was generated using MicrobeJ plugin for ImageJ, with the one pole oriented at 0.0 and the other at 1.0.[72]

Table 2: DNA oligos.

Name	Description
SEW72	cggcatggacgagctgtacaagggtagtgccggatctgccgccggaagcggcgagtttggcgagattgc
SEW82	gctattaaacaagggtatgggggtagtgccggatctgccgccggaagcggcgagtttgtgagcaagggcgaggagc
SEW89	tcatggagagcgacgccagtggtagtgccg
SEW90	ggagagcgacgccagtggtagtgccggatctgccgccggaagcggcgagtttgtgagcaagggcgaggagc
SEW110	gtatattagttaagtataagaaggagatatacatatggtgagcaagggcgaggagc
SEW112	cgagctgtacaagggtagtgccggatctgccgccggaagcggcgagtttggcgagattgctgcccttaagc
SEW113	gcggctattaaacaagggtatgggtaaatggcagatctcaattggatatcggc
SEW114	gtatattagttaagtataagaaggagatatacatatgggcgagattgctgccct
SEW115	gcggctattaaacaagggtatgggggtagtgccggatctgccgccggaagcggcgagtttgtgagcaagggc
SEW116	acaagggtatgggggtagtgccggatctgccgccggaagcggcgagtttgtgagcaagggcgaggagc
SEW117	cggcatggacgagctgtacaagtaaatggcagatctcaattggatatcggc
SEW118	gtatattagttaagtataagaaggagatatacatatgagtggggacttagaaaatgaagtagcgc
SEW119	gtcatggagagcgacgccagtggtagtgccggatctgccgccggaagcggcgagtttgtgagcaagggcg
SEW120	aagcggcgagtttgtgagcaagggcgaggagc
SEW148	cctgaaaaatactgttatggaatccgatgcttccggtagtgccggat
SEW189	gtatattagttaagtataagaaggagatatacatatgggcagcgctggttctg
SEW198	gtcatggagtctgacgccagcggtagtgccg
SEW199	ggagtctgacgccagcggtagtgccggatctgccgccggaagcggcgagtttgtgagcaagggcgaggagc
SEW193	gtatattagttaagtataagaaggagatatacatatgtcgggtgacttggaaaacgagg
SEW202	Ggctgcgggtagtggcgagtttggtagtgccggat

SEW203	gtagtggcgagtttggtagtgccggatctgccgccggaagcggcgagtttgtgagcaagggcgaggagc
SEW248	atccgatgcttccggtagtgccggatctgccgccggaagcggcgagtttgtgagcaagggcgaggagc
SEW302	cgccggaagcggcgagtttatggtgagcaagg
SEW303	gaagcggcgagtttatggtgagcaagggcgaggagc
SEW319	gtatattagttaagtataagaaggagatatacatatgaaaatcgctgcgctgaagg
SEW416	gtatattagttaagtataagaaggagatatacatatgtcgggcgatcttgagaacg
SEW417	cactgttatggagagtgatgcttccggtagtgccggat
SEW418	gagtgatgcttccggtagtgccggatctgccgccggaagcggcgagtttgtgagcaagggcgaggagc

Table 3: Gene blocks.

Name	Description	Reference
HB2-Waldo8x-HB3	atgggcgagattgctgcccttaagcaagagatcgccgcgttaaaaaaggaaaatgctgcgctgaagtgggaaatcgcagcattgaagcagggctactatggcagcgctggttctgcggcgggttccggcgagttcggttccgccggttcagcagctgggagcggtgagttcgggtctgcgggttcggcagccgggagtggagaatttggttccgccgggtccgccgccggatcgggtgaattcggatcggcaggttcggctgcgggcagtggtgaatttggttcagccggaagcgcggcaggatccggtgaattcgggagcgcagggtccgctgcagggtcgggagagtttgggtcagctggatcggctgcgggtagtggcgagtttgggaaattgccgctatcaaacaggagatagcggctataaaaaaggagatcgcagctattaaatgggagatagcggctattaaacaagggtatggg	This Study
HB4-Waldo8x-HB5	atgagtggggacttagaaaatgaagtagcgcaattagaacgggaagtgagatcacttgaggatgaggcagccgagctggaacaaaaggtttcccgcttgaaaaacgagatagaagacttgaaggcggagggcagcgctggttctgcggcgggttccggcgagttcggttccgccggttcagcagctgggagcggtgagttcgggtctgcgggttcggcagccgggagtggagaatttggttccgccgggtccgccgccggatcgggtgaattcggatcggcaggttcggctgcgggcagtggtgaatttggttcagccggaagcgcggcaggatccggtgaattcgggagcgcagggtccgctgcagggtcgggagagtttgggtcagctggatcggctgcgggtagtggcgagtttgcccctcagatgctgagagaacttcaagaaaccaatgcggccttacaggacgttcgggagttgttgcgccagcaggtcaaagagataaccttcttaaagaataccgtcatggagagcgacgccagt	This Study
HB2-Waldo4x-HB3	atgggcgagattgctgcccttaagcaagagatcgccgcgttaaaaaaggaaaatgctgcgctgaagtgggaaatcgcagcattgaagcagggctactatggtagtgcaggttctgctgcaggttctggtgaatttggctccgctgggtcagcagcaggatctggggagtttgggagtgcaggttcagcggcaggctctggcgagttcggttcggctggctccgcagccggaagcggtgaattcgggggaaattgccgctatcaaacaggagatagcggctataaaaaaggagatcgcagctattaaatggggagatagcggctattaaacaagggtatggg	This Study
HB4-Waldo4x-HB5	atgagtggggacttagaaaatgaagtagcgcaattagaacgggaagtgagatcacttgaggatgaggcagccgagctggaacaaaaggtttcccgcttgaaaaacgagatagaagacttgaaggcggagggtagtgcaggttctgctgcaggttctggtgaatttggctccgctgggtcagcagcaggatctggggagtttgggagtgcaggttcagcggcaggctctggcgagttcggttcggctggctccgcagccggaagcggtgaattcgcccctcagatgctgagagaacttcaagaaaccaatgcggccttacaggacgttcgggagttgttgcgccagcaggtcaaagagataaccttcttaaagaataccgtcatggagagcgacgccagt	This Study
Waldo8x-HB4-HB5-Waldo1x	atgggcagcgctggttctgcggcgggttccggcgagttcggttccgccggttcagcagctgggagcggtgagttcgggtctgcgggttcggcagccgggagtggagaatttggttccgccgggtccgccgccggatcgggtgaattcggatcggcaggttcggctgcgggcagtggtgaatttggttcagccggaagcgcggcaggatccggtgaattcgggagcgcagggtccgctgcagggtcgggagagtttgggtcagctggatcggctgcgggtagtggcgagtttatgtcgggtgacttggaaaacgaggtggcacaattagagagagaagttcgcagcctggaggatgaggctgctgaacttgagcagaaagtttcgagattgaaaaacgaaatagaggaccttaaagccgaagcccctcaaatgttacgggagctgcaggaaacgaacgcggcactgcaggatgtccgggagctgctgagacaacaagtaaaagaaataaccttctcttaaaaacacagtcatggagtctgacgccagcggtagtgccggatctgccgccggaagcggcgagttt	This Study

HB4-HB5-Waldo9x	atgtcgggtgacttggaaaacgaggtggcacaattagagagagaagttcgc agcctggaggatgaggctgctgaacttgagcagaaagtttcgagattgaaaa acgaaatagaggaccttaaagccgaagcccctcaaatgttacgggagctgc aggaaacgaacgcggcactgcaggatgtccgggagctgctgagacaacaa gtaaaagaaataacctttcttaaaaacacagtcatggagtctgacgccagcat gggcagcgctggttctgcggcgggttccggcgagttcggttccgccggttc agcagctgggagcggtgagttcgggtctgcgggttcggcagccgggagtg gagaatttggttccgccgggtccgccgccggatcgggtgaattcggatcgg caggttcggctgcgggcagtggtgaatttggttcagccggaagcgcggcag gatccggtgaattcgggagcgcagggtccgctgcagggtcgggagagtttg ggtcagctggatcggctgcgggtagtggcgagtttggtagtgccggatctgc cgccggaagcggcgagttt	This Study
HB4-Waldo1x-E3- Waldo2x-E3- Waldo1x-HB5	atgtcaggggatttagaaaacgaggtagcccaacttgaacgggaagtaaga agcttggaggacgaggctgcggaactggaacaaaaagtctctcgccttaag aatgaaatagaagacctgaaagcagaggggtccgccggctctgcagcggg tagcggagagtttgaaatcgccgcgttagaaaaagaaatcgcagccttggaa aaagaaattgcggcccttgagaagggatcggctggttccgctgcggggtca ggtgagtttgggtcggctggatcagccgctggttccggcgagtttgagatag ctgcattagaaaaggagattgccgcgttagaaaaggagattgccgccttgga aaaggggtccgccggtagtgccgcaggatcaggtgaatttgcgccacaaat gcttcgcgaattacaagaaactaatgccgcccttcaagacgtacgcgagttgt tgcggcagcaagtaaaggaaatcaccttcctgaaaaatactgttatggaatcc gatgcttcc	This Study
HB4-Waldo1x-K3- Waldo2x-K3- Waldo1x-HB5	atgtcgggcgatcttgagaacgaagtcgcgcaactggaacgcgaggttcgc agcctggaagacgaagcggctgagttggagcaaaaggtgtcgcggctgaa aaatgagatagaggatttaaaggccgaaggttcggcaggatctgcggcggg atccggtgagttcaaaattgccgcgcttaaggaaaaaattgcggctctgaag gagaagattgcggctcttaaggagggaagtgctggatctgcggcaggttcc ggcgagtttggatcagcgggaagcgcggcgggctcgggcgagtttaaaat agccgcgttaaaagagaaaatagctgcccttaaagagaaaattgcagcatta aaagaagggagcgcgggcagtgccgccgggtcaggagaattcgctccac agatgttaagagagcttcaggaaactaacgctgcattacaggacgtgagaga gttattgcgtcaacaagttaaggagatcactttcttaaaaaacactgttatggag agtgatgcttcc	This Study
K3-Waldo1x-Venus	atgaaaatcgctgcgctgaaggaaaaaatagctgctctgaaagagaaaatcg ccgctcttaaagaaggtagtgccggatctgccgccggaagcggcgagtttat ggtgagcaagggcgaggagctgttcaccggggtggtgcccatcctggtcg agctggacggcgacgtaaacggccacaagttcagcgtgtccggcgagggc gagggcgatgccacctacggcaagctgaccctgaagctgatctgcaccacc ggcaagctgcccgtgccctggcccaccctcgtgaccaccctgggctacggc ctgcagtgcttcgcccgctaccccgaccacatgaagcagcacgacttcttca agtccgccatgcccgaaggctacgtccaggagcgcaccatcttcttcaagga cgacggcaactacaagacccgcgccgaggtgaagttcgagggcgacacc ctggtgaaccgcatcgagctgaagggcatcgacttcaaggaggacggcaa catcctggggcacaagctggagtacaactacaacagccacaacgtctatatc accgccgacaagcagaagaacggcatcaaggccaacttcaagatccgcca caacatcgaggacggcggcgtgcagctcgccgaccactaccagcagaaca ccccccatcggcgacggccccgtgctgctgcccgacaaccactacctgagct accagtccgccctgagcaaagaccccaacgagaagcgcgatcacatggtc ctgctggagttcgtgaccgccgccgggatcactctcggcatggacgagctgt acaagtaa	This Study

Table 4: Plasmids.

Plasmid	Description	Reference
pCZ221	pACYCDuet1-GFP	Chao Zhang
pJH42	pACYCDuet1-mCherry-PopZ	[44]
pSEW34	pCDFDuet1-eCFP-HB2-Waldo8x-HB3	This Study
pSEW35	pCDFDuet1-HB2-Waldo8x-CC-HB3-eCFP	This Study
pSEW37	pCDFDuet1-HB4-Waldo8x-HB5-eCFP	This Study
pSEW90	pCDFDuet1-HB4-Waldo4x-HB5-eCFP	This Study
pSEW91	pCDFDuet1-HB2-Waldo4x-HB3-eCFP	This Study
pSEW70	pCDFDuet1-Waldo8x-HB4-HB5-Waldo1x-eCFP	This Study
pSEW71	pCDFDuet1-HB4-HB5-Waldo9x-eCFP	This Study
pSEW93	pCDFDuet1-HB4-Waldo1x-E3-Waldo2x-E3-Waldo1x-HB5-eCFP	This Study

pSEW191	pCDFDuet1-HB4-Waldo1x-K3-Waldo2x-K3-Waldo1x-HB5-eCFP	This Study
pSEW143	pACYCDuet1-K3-Waldo1x-Venus	This Study

Bibliography

1 Oparin AI. Proiskhozhdenie zhizny 1924.

2 Miller SL, William Schopf J, Lazcano A. Oparin's 'origin of life': Sixty years later. *J Mol Evol* 1997;**44**:351–3. https://doi.org/10.1007/PL00006153.

3 Stanley L . Miller. A Production of Amino Acids under Possible Primitive Earth Conditions. *Science (80-)* 1953;**117**:528–9.

4 Dubin P, Stewart RJ. Complex coacervation. *Soft Matter* 2018:329–30. https://doi.org/10.1039/c7sm90206a.

5 Evreinova TN, Mamontova TW, Karnauhov VN, Stephanov SB, Hrust UR. Coacervate systems and origin of life. *Orig Life* 1974;**5**:201–5. https://doi.org/10.1007/BF00927024.

6 Brangwynne CP, Hyman AA. In Retrospect: The Origin of Life. *Nature* 2012;**491**:524–5.

7 HERSHEY AD, CHASE M. Independent functions of viral protein and nucleic acid in growth of bacteriophage. *J Gen Physiol* 1952;**36**:39–56. https://doi.org/10.1085/jgp.36.1.39.

8 Oparin AI. A.N. Bach Institute of Biochemistry, Leninsky pr. 33, Moscow, U.S.S.R. *Orig Life* 1976;**7**:3–8.

9 Fox SW. A theory of macromolecular and cellular origins. *Nature* 1965;**205**:328–40. https://doi.org/10.1038/205328a0.

10 Grote M. Jeewanu, or the 'particles of life' : the approach of Krishna Bahadur in 20th century origin of life research. *J Biosci* 2011:563–70. https://doi.org/10.1007/s12038-011-9087-0.

11 Bahadur K. Synthesis of Jeewanu, the Protocell. *Zentralblatt Fur Bakteriol Parasitenkunde, Infekt Und Hyg Zweite Naturwissenschaftliche Abt Allg Landwirtsch Und Tech Mikrobiol* 1967;**121**:291–319.

12 Caren LD, Ponnamperuma C. A review of some experiments on the synthesis of 'Jeewanu'. *NASA Intern Notes* 1967;**55**:1–6.

13 Brangwynne CP, Eckmann CR, Courson DS, Rybarska A, Hoege C, Gharakhani J, *et al.* Germline P Granules Are Liquid Droplets That Localize by Controlled Dissolution/Condensation. *Science (80-)* 2009;**324**:1729–32. https://doi.org/10.1126/science.1171716.

14 Updike D, Strome S. P Granule Assembly and Function in Caenorhabditis Elegans Germ

Cells.

15 Hird SN, White JG. Cortical and cytoplasmic flow polarity in early embryonic cells of Caenorhabditis elegans. *J Cell Biol* 1993;**121**:1343–55. https://doi.org/10.1083/jcb.121.6.1343.

16 Kato M, Han TW, Xie S, Shi K, Du X, Wu LC, *et al.* Cell-free formation of RNA granules: Low complexity sequence domains form dynamic fibers within hydrogels. *Cell* 2012;**149**:753–67. https://doi.org/10.1016/j.cell.2012.04.017.

17 Li P, Banjade S, Cheng HC, Kim S, Chen B, Guo L, *et al.* Phase transitions in the assembly of multivalent signalling proteins. *Nature* 2012;**483**:336–40. https://doi.org/10.1038/nature10879.

18 Banani SF, Lee HO, Hyman AA, Rosen MK. Biomolecular condensates: Organizers of cellular biochemistry. *Nat Rev Mol Cell Biol* 2017;**18**:285–98. https://doi.org/10.1038/nrm.2017.7.

19 Nott TJ, Petsalaki E, Farber P, Jervis D, Fussner E, Plochowietz A, *et al.* Phase Transition of a Disordered Nuage Protein Generates Environmentally Responsive Membraneless Organelles. *Mol Cell* 2015;**57**:936–47. https://doi.org/10.1016/j.molcel.2015.01.013.

20 Shapiro L, McAdams HH, Losick R. Why and how bacteria localize proteins. *Sci (New York, NY)* 2009;**326**:1225–8. https://doi.org/10.1126/science.1175685.

21 Laloux G, Jacobs-Wagner C. How do bacteria localize proteins to the cell pole? *J Cell Sci* 2014;**127**:11–9. https://doi.org/10.1242/jcs.138628.

22 Alley MRK, Maddock JR, Shapiro L. Polar localization of a bacterial chemoreceptor. *Genes Dev* 1992;**6**:825–36. https://doi.org/10.1101/gad.6.5.825.

23 Erfei B, Lutkenhaus J. FtsZ ring structure associated with division in Escherichia coli. *Nature* 1991;**354**:161–3.

24 Werner JN, Chen EY, Guberman JM, Zippilli AR, Irgon JJ, Gitai Z. Quantitative genome-scale analysis of protein localization in an asymmetric bacterium. *Proc Natl Acad Sci U S A* 2009;**106**:7858–63. https://doi.org/10.1073/pnas.0901781106.

25 dos Santos VT, Bisson-Filho AW, Gueiros-Filho FJ. DivIVA-mediated polar localization of ComN, a posttranscriptional regulator of Bacillus subtilis. *J Bacteriol* 2012;**194**:3661–9. https://doi.org/10.1128/JB.05879-11.

26 Lenarcic R, Halbedel S, Visser L, Shaw M, Wu LJ, Errington J, *et al.* Localisation of DivIVA by targeting to negatively curved membranes. *EMBO J* 2009;**28**:2272–82. https://doi.org/10.1038/emboj.2009.129.

27 Ebersbach G, Briegel A, Jensen GJ, Jacobs-Wagner C. A Self-Associating Protein Critical for Chromosome Attachment, Division, and Polar Organization in Caulobacter. *Cell*

2008;**134**:956–68. https://doi.org/10.1016/j.cell.2008.07.016.

28 Laloux G, Jacobs-Wagner C. Spatiotemporal control of PopZ localization through cell cycle-coupled multimerization. *J Cell Biol* 2013;**201**:827–41. https://doi.org/10.1083/jcb.201303036.

29 Al-Husini N, Tomares DT, Bitar O, Childers WS, Schrader JM. α-Proteobacterial RNA Degradosomes Assemble Liquid-Liquid Phase-Separated RNP Bodies. *Mol Cell* 2018;**71**:1027-1039.e14. https://doi.org/10.1016/j.molcel.2018.08.003.

30 Cohan MC, Pappu R V. Making the Case for Disordered Proteins and Biomolecular Condensates in Bacteria. *Trends Biochem Sci* 2020;**45**:668–80. https://doi.org/10.1016/j.tibs.2020.04.011.

31 Ladouceur AM, Parmar BS, Biedzinski S, Wall J, Tope SG, Cohn D, *et al.* Clusters of bacterial RNA polymerase are biomolecular condensates that assemble through liquid-liquid phase separation. *Proc Natl Acad Sci U S A* 2020;**117**:18540–9. https://doi.org/10.1073/pnas.2005019117.

32 Jalal ASB, Le TBK. Bacterial chromosome segregation by the ParABS system: Chromosome segregation by ParAB-parS. *Open Biol* 2020;**10**:. https://doi.org/10.1098/rsob.200097rsob200097.

33 Guilhas B, Walter JC, Rech J, David G, Walliser NO, Palmeri J, *et al.* ATP-Driven Separation of Liquid Phase Condensates in Bacteria. *Mol Cell* 2020;**79**:293-303.e4. https://doi.org/10.1016/j.molcel.2020.06.034.

34 Skerker JM, Laub MT. Cell-cycle progression and the generation of asymmetry in Caulobacter crescentus. *Nat Rev Microbiol* 2004;**2**:325–37. https://doi.org/10.1038/nrmicro864.

35 Ebersbach G, Briegel A, Jensen GJ, Jacobs-Wagner C. A Self-Associating Protein Critical for Chromosome Attachment, Division, and Polar Organization in Caulobacter. *Cell* 2008;**134**:956–68. https://doi.org/10.1016/j.cell.2008.07.016.

36 Lasker K, von Diezmann L, Zhou X, Ahrens DG, Mann TH, Moerner WE, *et al.* Selective sequestration of signalling proteins in a membraneless organelle reinforces the spatial regulation of asymmetry in Caulobacter crescentus. *Nat Microbiol* 2020;**5**:418–29. https://doi.org/10.1038/s41564-019-0647-7.

37 Yeong V (Columbia U, Werth E (Columbia U, Brown L (Columbia U, Obermeyer A (Columbia U. Formation of biomolecular condensates in bacteria by tuning protein electrostatics. *BioRxiv* n.d. https://doi.org/https://doi.org/10.1101/2020.05.02.072645.

38 Guo H, Ryan JC, Mallet A, Song X, Pabst V, Decrulle A, *et al.* Spatial engineering of E. coli with addressable phase-separated RNAs. *BioRxiv* 2020:2020.07.02.182527.

39 Mushnikov N V., Fomicheva A, Gomelsky M, Bowman GR. Inducible asymmetric cell

division and cell differentiation in a bacterium. *Nat Chem Biol* 2019;**15**:925–31. https://doi.org/10.1038/s41589-019-0340-4.

40 Molinari S, Shis DL, Bhakta SP, Chappell J, Igoshin OA, Bennett MR. A synthetic system for asymmetric cell division in Escherichia coli. *Nat Chem Biol* 2019;**15**:917–24. https://doi.org/10.1038/s41589-019-0339-x.

41 Lim HC, Bernhardt TG. A PopZ-linked apical recruitment assay for studying protein–protein interactions in the bacterial cell envelope. *Mol Microbiol* 2019;**112**:1757–68. https://doi.org/10.1111/mmi.14391.

42 Bowman GR, Comolli LR, Zhu J, Eckart M, Koenig M, Downing KH, *et al.* A Polymeric Protein Anchors the Chromosomal Origin/ParB Complex at a Bacterial Cell Pole. *Cell* 2008;**134**:945–55. https://doi.org/10.1016/j.cell.2008.07.015.

43 Shen W, Zhang K, Kornfield JA, Tirrell DA. Tuning the erosion rate of artificial protein hydrogels through control of network topology. *Nat Mater* 2006;**5**:153–8. https://doi.org/10.1038/nmat1573.

44 Holmes JA, Follett SE, Wang H, Meadows CP, Varga K, Bowman GR. Caulobacter PopZ forms an intrinsically disordered hub in organizing bacterial cell poles. *Proc Natl Acad Sci* 2016;**113**:12490–5. https://doi.org/10.1073/pnas.1602380113.

45 Bowman GR, Perez AM, Ptacin JL, Ighodaro E, Folta-Stogniew E, Comolli LR, *et al.* Oligomerization and higher-order assembly contribute to sub-cellular localization of a bacterial scaffold. *Mol Microbiol* 2013;**90**:776–95. https://doi.org/10.1111/mmi.12398.

46 Petka WA. Reversible Hydrogels from Self-Assembling Artificial Proteins. *Science (80-)* 1998;**281**:389–92. https://doi.org/10.1126/science.281.5375.389.

47 Truebestein L, Leonard TA. Coiled-coils: The long and short of it. *BioEssays* 2016;**38**:903–16. https://doi.org/10.1002/bies.201600062.

48 Burkhard P, Stetefeld J, Strelkov S V. Coiled coils: A highly versatile protein folding motif. *Trends Cell Biol* 2001;**11**:82–8. https://doi.org/10.1016/S0962-8924(00)01898-5.

49 Kohn WD, Hodges RS. De novo design of α-helical coiled coils and bundles: Models for the development of protein-design principles. *Trends Biotechnol* 1998;**16**:379–89. https://doi.org/10.1016/S0167-7799(98)01212-8.

50 Dakhara SL, Anajwala CC. Polyelectrolyte complex: A pharmaceutical review. *Syst Rev Pharm* 2010;**1**:121–7. https://doi.org/10.4103/0975-8453.75046.

51 Waldo GS, Standish BM, Berendzen J, Terwilliger TC. Rapid protein-folding assay using green fluorescent protein. *Nat Biotechnol* 1999;**17**:691–5. https://doi.org/10.1038/10904.

52 Dosztányi Z, Chen J, Dunker AK, Simon I, Tompa P. Disorder and sequence repeats in hub proteins and their implications for network evolution. *J Proteome Res* 2006;**5**:2985–95.

https://doi.org/10.1021/pr060171o.

53 Pak CW, Kosno M, Holehouse AS, Padrick SB, Mittal A, Ali R, *et al.* Sequence Determinants of Intracellular Phase Separation by Complex Coacervation of a Disordered Protein. *Mol Cell* 2016;**63**:72–85. https://doi.org/10.1016/j.molcel.2016.05.042.

54 Crabtree MD, Holland J, Kompella P, Babl L, Turner N, Baldwin AJ, *et al.* Repulsive electrostatic interactions modulate dense and dilute phase properties of biomolecular condensates. *BioRxiv* 2020:2020.10.29.357863.

55 Malashkevich VN, Kammerer RA, Efimov VP, Schulthess T, Engel J. The Crystal Structure of a Five-Stranded Coiled Coil in COMP: A Prototype Ion Channel? *Science (80-)* 1996;**274**:761–5. https://doi.org/10.1126/science.274.5288.761.

56 Fletcher JM, Boyle AL, Bruning M, Bartlett SgJ, Vincent TL, Zaccai NR, *et al.* A basis set of de novo coiled-Coil peptide oligomers for rational protein design and synthetic biology. *ACS Synth Biol* 2012;**1**:240–50. https://doi.org/10.1021/sb300028q.

57 Thomas F, Boyle AL, Burton AJ, Woolfson DN. A set of de novo designed parallel heterodimeric coiled coils with quantified dissociation constants in the micromolar to sub-nanomolar regime. *J Am Chem Soc* 2013;**135**:5161–6. https://doi.org/10.1021/ja312310g.

58 de Boer PAJ. Advances in understanding E. coli cell fission. *Curr Opin Microbiol* 2010;**13**:730–7. https://doi.org/10.1016/j.mib.2010.09.015.

59 Chai Q, Singh B, Peisker K, Metzendorf N, Ge X, Dasgupta S, *et al.* Organization of ribosomes and nucleoids in escherichia coli cells during growth and in quiescence. *J Biol Chem* 2014;**289**:11342–52. https://doi.org/10.1074/jbc.M114.557348.

60 Bowman GR, Comolli LR, Gaietta GM, Fero M, Hong SH, Jones Y, *et al.* Caulobacter PopZ forms a polar subdomain dictating sequential changes in pole composition and function. *Mol Microbiol* 2010;**76**:173–89. https://doi.org/10.1111/j.1365-2958.2010.07088.x.

61 Saberi S, Emberly E. Chromosome driven spatial patterning of proteins in bacteria. *PLoS Comput Biol* 2010;**6**:. https://doi.org/10.1371/journal.pcbi.1000986.

62 Rinas U, Garcia-Fruitós E, Corchero JL, Vázquez E, Seras-Franzoso J, Villaverde A. Bacterial Inclusion Bodies: Discovering Their Better Half. *Trends Biochem Sci* 2017;**42**:726–37. https://doi.org/10.1016/j.tibs.2017.01.005.

63 Fernandez-Rodriguez J, Marlovits TC. Induced heterodimerization and purification of two target proteins by a synthetic coiled-coil tag. *Protein Sci* 2012;**21**:511–9. https://doi.org/10.1002/pro.2035.

64 Thompson KE, Bashor CJ, Lim WA, Keating AE. Synzip protein interaction toolbox: In vitro and in vivo specifications of heterospecific coiled-coil interaction domains. *ACS Synth Biol* 2012;**1**:118–29. https://doi.org/10.1021/sb200015u.

65 Rapp PB, Omar AK, Shen JJ, Buck ME, Wang ZG, Tirrell DA. Analysis and Control of Chain Mobility in Protein Hydrogels. *J Am Chem Soc* 2017;**139**:3796–804. https://doi.org/10.1021/jacs.6b13146.

66 Jiang XR, Chen GQ. Morphology engineering of bacteria for bio-production. *Biotechnol Adv* 2016;**34**:435–40. https://doi.org/10.1016/j.biotechadv.2015.12.007.

67 Caccamo PD, Brun Y V. The Molecular Basis of Noncanonical Bacterial Morphology. *Trends Microbiol* 2018;**26**:191–208. https://doi.org/10.1016/j.tim.2017.09.012.

68 Typas A, Banzhaf M, Gross CA, Vollmer W. From the regulation of peptidoglycan synthesis to bacterial growth and morphology. *Nat Rev Microbiol* 2012;**10**:123–36. https://doi.org/10.1038/nrmicro2677.

69 Dressaire C, Neves Moreira R, Barahona S, Alves de Matos AP, Arraiano CM. BolA Is a Transcriptional Switch That Turns Off Motility and Turns. *MBio* 2015;**6**:1–13. https://doi.org/10.1128/mBio.02352-14.Editor.

70 Gibson DG, Young L, Chuang R-Y, Venter JC, Hutchison C a, Smith HO, *et al.* Enzymatic assembly of DNA molecules up to several hundred kilobases. *Nat Methods* 2009;**6**:343–5. https://doi.org/10.1038/nmeth.1318.

71 Hillson NJ, Rosengarten RD, Keasling JD. J5 DNA assembly design automation software. *ACS Synth Biol* 2012;**1**:14–21. https://doi.org/10.1021/sb2000116.

72 Ducret A, Quardokus EM, Brun Y V. MicrobeJ, a tool for high throughput bacterial cell detection and quantitative analysis. *Nat Microbiol* 2016. https://doi.org/10.1038/nmicrobiol.2016.77.